The control was designed to have no target and no significant biological activity, except in reticulocytes from humans with thalassemia who have a splice-generating mutation at position 705 in β-globin pre-mRNA. The delivery procedure was performed according to the recommendations of Gene Tools. The delivery formulation consisted of a prepared duplex of PMO and partially complimentary DNA oligomer together with a weakly basic delivery reagent (ethoxylated polyethylenimine). Because the morpholino oligomers are stable and nuclease resistant, there was no need to repeat the delivery procedure.

AsPC-1 cells were treated with FLIP antisense PMO and control PMO for 2 d. The delivery mixture was an aqueous solution of 0.5 mM FLIP antisense PMO or 0.5 mM control PMO and morpholino/DNA stock solution (Gene Tools). To this was added 200 μM ethoxylated polyethylenimine special delivery solution, followed by vortexing and incubation at room temperature for 20 min to generate the complete delivery solution. Then the medium was removed and the solution was added to cells, which were placed into a CO_2 incubator. After 3 h, the delivery solution was aspirated and replaced with fresh serum-containing medium.

Statistical Analysis

Results are presented as the mean ± SD. Data were analyzed by Student's *t*-test, and statistical significance was accepted at a *P*-value of less than 0.05. Differences among three groups were assessed by analysis of variance, followed by a post hoc Tukey-Kramer test when appropriate. Each experiment was repeated independently at least three times.

RESULTS

Effect of Smac Peptide on TRAIL-Induced Apoptosis of Pancreatic Cancer Cells

The effect of Smac peptide on TRAIL-induced apoptosis was determined for various pancreatic cancer cell lines. We investigated whether this cell-permeable synthetic peptide containing the four N-terminal residues essential for XIAP inactivation could induce apoptosis, while the control peptide was a reversed version of Smac bound to arginine repeats.

Treatment with TRAIL in the presence of Smac peptide resulted in a significant increase of cell death in a dose-dependent manner for the Suit-2, CFPAC-1, Panc-1, and BxPC-3 cell lines (Fig. 1). However, TRAIL had no effect on TRAIL-resistant AsPC-1 cells, which strongly overexpress FLIP-S, even in the presence of Smac peptide.

Effect of FLIP Antisense on TRAIL-Induced Apoptosis of AsPC-1 Cells

Next, we tested whether direct down-regulation of FLIP by FLIP antisense could restore TRAIL sensitivity to TRAIL-resistant AsPC-1 cells. Cells were treated with FLIP antisense or control oligonucleotides and subsequently exposed to various concentrations of TRAIL. We found that treatment with FLIP antisense could suppress the expression of FLIP-L and FLIP-S in AsPC-1 cells (Fig. 2A). In addition, TRAIL induced cell death in the presence of FLIP antisense, although the effect on cell viability was relatively modest (Fig. 2B).

Effect of Combined Use of FLIP Antisense and Smac Peptide on TRAIL-Induced Apoptosis of AsPC-1 Cells

To modulate the TRAIL resistance of AsPC-1 cells, we tested the combination FLIP antisense and Smac

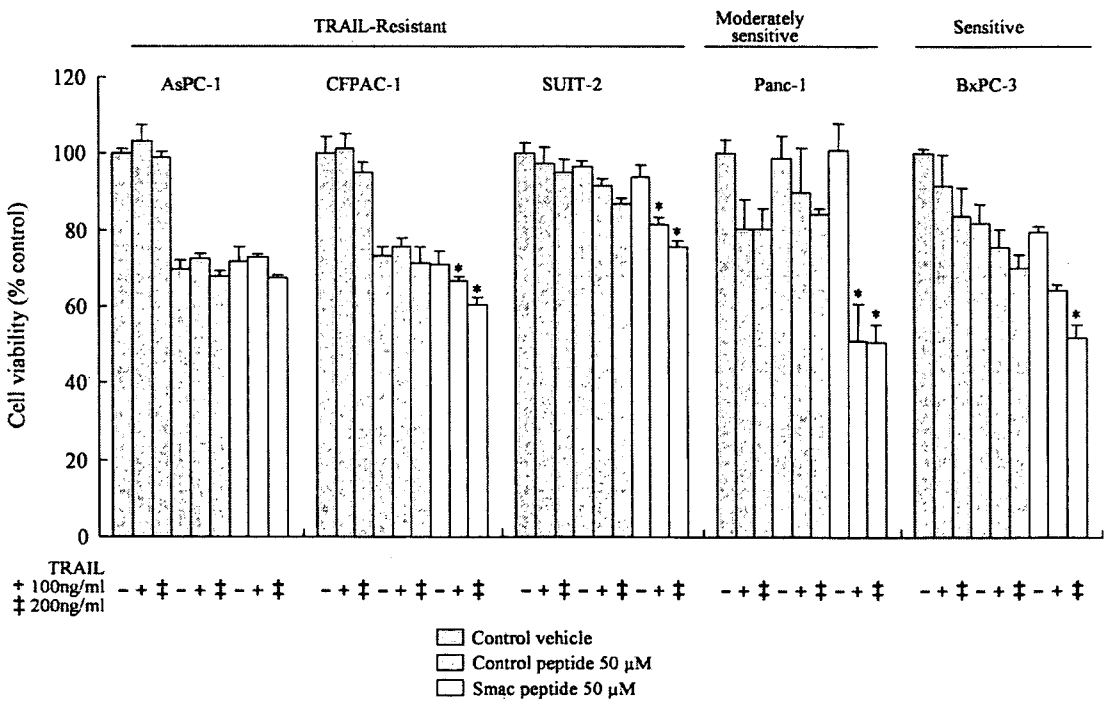

FIG. 1. Effect of Smac-peptide on TRAIL-induced apoptosis of pancreatic cancer cells. Cells were treated with various concentrations of TRAIL for 48 h in the presence of Smac peptide or the control peptide. Cell viability is shown as the mean percentage compared with untreated cells and bars represent the SD (n = 3). *, $P < 0.05$ for control peptide *versus* Smac peptide.

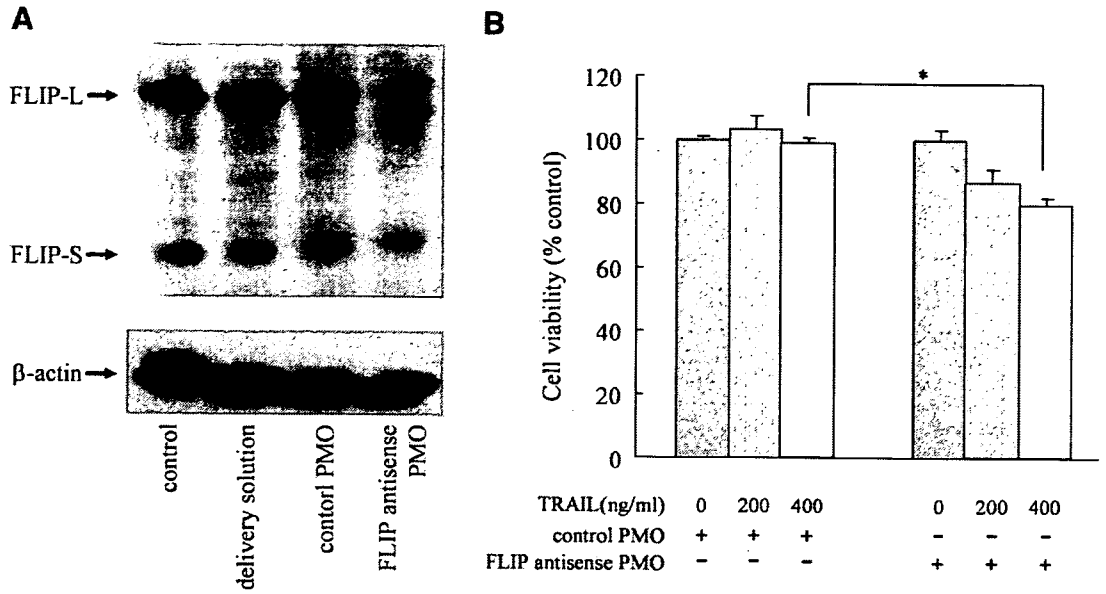

FIG. 2. Effect of FLIP antisense on FLIP expression and TRAIL sensitivity of TRAIL-resistant AsPC-1 cells. (A) Expression of FLIP-L and FLIP-S by immunoblot analysis with anti-FLIP monoclonal antibody. Expression of both FLIP-L and FLIP-S was decreased by FLIP antisense PMO. β-Actin was used to verify equal loading of proteins. (B) AsPC-1 cells were treated with TRAIL (0, 200, or 400 ng/mL) for 24 h after pretreatment with control PMO or FLIP antisense PMO. Cell viability is shown as the mean percentage compared with untreated cells and bars represent the SD ($n = 3$). *, $P < 0.05$ for control PMO *versus* FLIP antisense PMO.

peptide. TRAIL caused apoptosis of AsPC-1 cells in the presence of both FLIP antisense and Smac peptide, and the improvement of sensitivity to TRAIL was greater than the additive effect of FLIP antisense plus Smac peptide (Fig. 3A).

Effect of Combined Use of FLIP Antisense and Embelin on TRAIL-Induced Apoptosis of AsPC-1 Cells

Because the combination of FLIP antisense and Smac peptide had an excellent effect, we next used the XIAP inhibitor embelin, which is derived from a natural benzoquinone product originally isolated from the Japanese herb Ardisia. We found that TRAIL effectively induced the death of AsPC-1 cells in the presence of FLIP antisense and embelin (Fig. 3B). Interestingly, embelin sensitized cells to TRAIL in a manner that was not dose-dependent.

Effect of FLIP Antisense Plus Smac Peptide on Caspases and PARP

We next investigated the modulation of intracellular signaling in TRAIL-resistant AsPC-1 cells by the combination of FLIP antisense and Smac peptide. Exposure to TRAIL did not induce processing of caspases or cleavage of PARP, and the same results were obtained in the presence of Smac peptide. In the presence of FLIP antisense, however, partial cleavage of caspases-3 and -8 was observed. In the presence of both FLIP antisense and Smac peptide, exposure to TRAIL induced strong activation of caspases-3 and -8 as well as cleavage of PARP (Fig. 4).

DISCUSSION

We have previously shown that TRAIL induces apoptosis to a variable extent in different pancreatic cancer cell lines [3]. Resistant cell lines (AsPC-1, CFPAC-1, and Suit-2) show strong expression of XIAP and FLIP, one of the splice variants of FLIP. Therefore, we investigated whether a Smac peptide containing the four N-terminal residues required for inactivation of XIAP or direct down-regulation of FLIP by using FLIP antisense could restore the sensitivity to apoptosis of TRAIL-resistant pancreatic cancer cells.

To address this question, we linked the six N-terminal residues of Smac protein to a cell membrane-penetrating polyarginine to facilitate intracellular delivery. Synthetic Smac N-terminal peptides fused to membrane-penetrating peptides have been found to bypass mitochondrial regulation and sensitize both cultured human cancer cells and tumor xenografts in mice [4–7]. In the presence of Smac peptide, TRAIL induced a significant and dose-dependent increase of the death of Suit-2, CFPAC-1, Panc-1, and BxPC-3 cells, but it showed no effect on TRAIL-resistant AsPC-1 cells which overexpress FLIP-S. Thus, AsPC-1 cells were still resistant to induction of apoptosis by TRAIL, even after inhibition of XIAP. These findings suggest that an additional block may be imposed by FLIP upstream of XIAP in

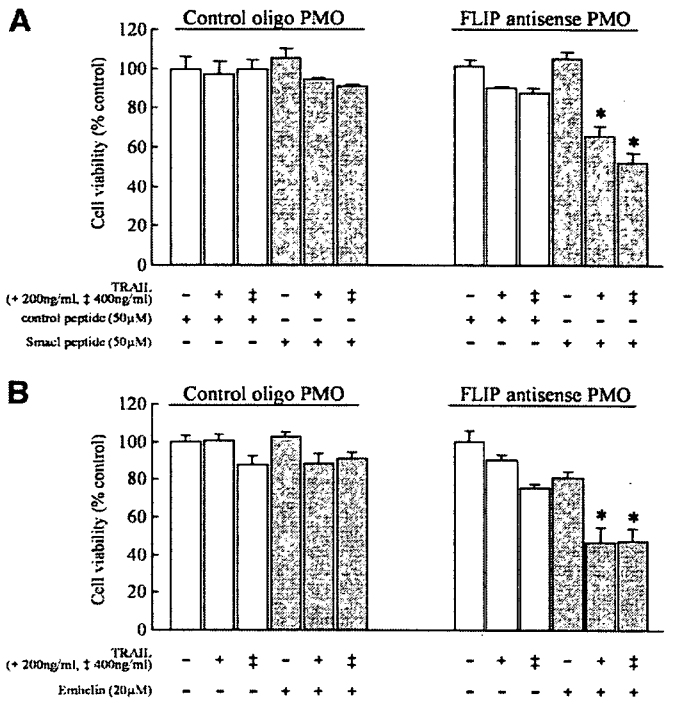

FIG. 3. Effect of combined treatment with FLIP antisense and Smac peptide (A) or FLIP antisense and embelin (B) on TRAIL-induced apoptosis of AsPC-1cells. (A) AsPC-1 cells were treated with TRAIL (0, 200, or 400 ng/mL) for 48 h after pretreatment with control PMO or FLIP antisense PMO with or without control peptide or Smac peptide (50 μM). *, $P < 0.05$ for Smac peptide *versus* control peptide. (B) AsPC-1 cells were treated with TRAIL (0, 200, or 400 ng/mL) for 48 h after pretreatment with control PMO or FLIP antisense PMO with or without embelin (20 μM). *, $P < 0.05$ for control *versus* embelin. Cell viability is shown as the mean percentage compared with untreated cells and bars represent the SD ($n = 3$).

these cells. Smac and the control peptide alone had a moderate toxic effect on AsPC-1, CFPAC-1, and BxPC-3 cells, possibly due to lysis by cell membrane-penetrating polyarginine.

Therefore, we next investigated whether direct down-regulation of FLIP by FLIP antisense could restore the sensitivity to apoptosis of TRAIL-resistant AsPC-1 cells. FLIP antisense suppressed the expression of both FLIP-L and FLIP-S by AsPC-1 cells, and it sensitized these cells to TRAIL-induced apoptosis, although the actual decrease of cell viability was relatively modest. Similar to our results, it has been reported that direct down-regulation of FLIP sensitizes several other cancer cell lines to TRAIL [8–10]. Since FLIP-S and FLIP-L cDNAs share considerable homology (up to 75%), it is technically difficult to design an antisense oligonucleotide for FLIP-S that does not interfere with expression of the long isoform. Thus, additional studies are needed to determine which FLIP isoform plays a more important role in regulating the TRAIL sensitivity of pancreatic cancer cells.

In the present study, we used FLIP antisense PMO to determine the effect of direct down-regulation of FLIP expression. Unlike phosphorothioate antisense oligonucleotides, PMO is a novel antisense oligomer that has a neutral backbone at physiological pH and consists of a six-membered morpholine ring [11]. The absence of any internucleoside charge allows PMO to avoid triggering the nonspecific effects associated with commonly used phosphorothioate oligonucleotides [12, 13]. The safety of PMO antisense agents has been established, and no serious adverse effects or deaths have been reported in animal models or clinical trials [14].

Because the effect of Smac or FLIP antisense on sensitivity to apoptosis was limited, we next tested the combination of FLIP antisense and Smac. As a result, AsPC-1 cells regained TRAIL sensitivity in the presence of FLIP antisense plus Smac peptide and the effect was stronger than the sum of that for FLIP antisense alone plus that for Smac peptide alone. We then tested embelin, a natural benzoquinone product that was originally isolated from the Japanese herb Ardisia. Embelin was found to compete with Smac peptide for binding to XIAP BIR3 protein and showed similar affinity to that of native Smac peptide. As shown in Fig. 3B, TRAIL induced apoptosis of resistant AsPC-1 cells in the presence of FLIP antisense plus embelin. Similar to our results, it was previously reported that embelin could sensitize XIAP-overexpressing Jurkat cells to etoposide-induced

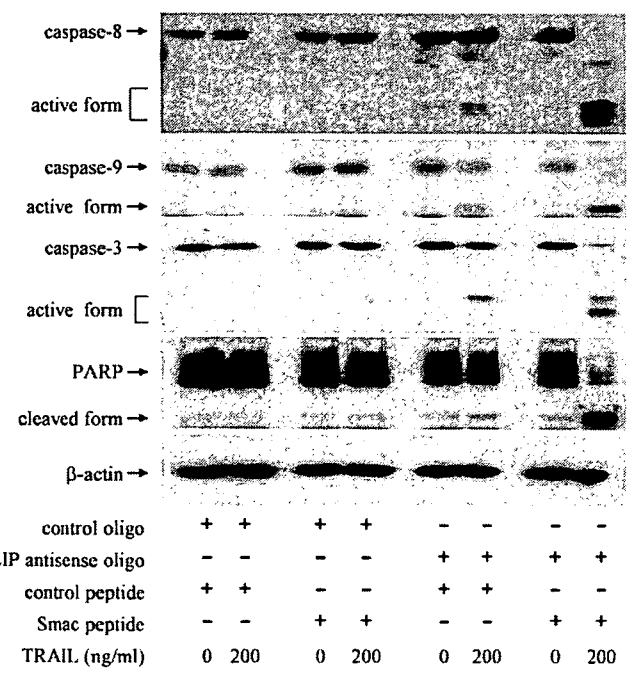

FIG. 4. Effect of combined FLIP antisense and Smac peptide on activation of caspases and cleavage of PARP. Activation of caspase-3, caspase-8, and caspase-9, as well as PARP cleavage, were determined by Western blot analysis of AsPC-1 cells after treatment with FLIP antisense plus Smac peptide. β-Actin was used to verify equal loading of proteins.

apoptosis [15]. Embelin is derived from a natural plant product, so it is easy to apply for clinical use. In addition, lower molecular weight compounds that mimic the action of Smac peptide could also be used clinically in combination with anticancer drugs.

XIAP has been identified as one of the most potent inhibitors of caspase activity and apoptosis [16]. Unlike Bcl-2 protein, which blocks the mitochondrial pathway of apoptosis, the antiapoptotic activity of XIAP is at least partly due to its ability to inhibit both mitochondrial-dependent and mitochondrial-independent apoptotic pathways by binding to and inhibiting the activation of initiator caspase-9, as well as the effector caspases (caspase-3 and -7), which are vital for the execution of apoptosis. FLIP is an intracellular antiapoptotic protein [17]. Although an inhibitory effect of FLIP on apoptosis induced by various stimuli has been demonstrated, its role in regulating the TRAIL sensitivity of pancreatic cancer cells has been unknown. Previous studies have shown that FLIP interrupts apoptotic signaling by interacting with FADD and caspase-8 to block caspase-8 activation, suggesting that the intracellular concentration of FLIP may determine the sensitivity of tumor cells to a variety of proapoptotic stimuli [18–21]. Therefore, regulation of XIAP and FLIP may be important for successful induction of apoptosis in TRAIL-resistant cancer cells. We have shown that TRAIL-resistant AsPC-1 cells were sensitized to TRAIL by FLIP antisense and Smac peptide, with proapoptotic caspases and PARP being activated (Fig. 4).

In conclusion, TRAIL-resistant pancreatic cancer cells can be transformed to TRAIL-sensitive cells by suppressing the expression of FLIP and XIAP. A low molecular weight XIAP inhibitor (embelin) combined with FLIP antisense was effective for restoring the sensitivity of TRAIL-resistant cells. These findings may provide useful information for TRAIL-based therapeutic strategies by restoring functional apoptotic pathways in pancreatic cancer cells. In addition, a small molecule such as embelin could be a lead compound for the development of effective XIAP inhibitors.

ACKNOWLEDGMENTS

This study was supported by a Grant-in-Aid (17390364) from the Ministry of Education, Culture, Sports, Science, and Technology of Japan.

REFERENCES

1. LeBlanc HN, Ashkenazi A. Apo2L/TRAIL and its death and decoy receptors. Cell Death Differ 2003;10:66.
2. Wang S, El-Deiry WS. TRAIL and apoptosis induction by TNF-family death receptors. Oncogene 2003;22:8628.
3. Mori T, Doi R, Toyoda E, et al. Regulation of the resistance to TRAIL-induced apoptosis as a new strategy for pancreatic cancer. Surgery 2005;138:71.
4. Fulda S, Wick W, Weller M, et al. Smac agonists sensitize for Apo2L/TRAIL- or anticancer drug-induced apoptosis and induce regression of malignant glioma in vivo. Nat Med 2002;8:808.
5. Yang L, Mashima T, Sato S, et al. Predominant suppression of apoptosome by inhibitor of apoptosis protein in non-small cell lung cancer H460 cells: Therapeutic effect of a novel polyarginine-conjugated Smac peptide. Cancer Res 2003;63:831.
6. Arnt CR, Chiorean MV, Heldebrant MP, et al. Synthetic Smac/DIABLO peptides enhance the effects of chemotherapeutic agents by binding XIAP and cIAP1 in situ. J Biol Chem 2002;277:44236.
7. Pei Z, Chu L, Zou W, et al. An oncolytic adenoviral vector of Smac increases antitumor activity of TRAIL against HCC in human cells and in mice. Hepatology 2004;39:1371.
8. Zhang X, Jin TG, Yang H, et al. Persistent c-FLIP(L) expression is necessary and sufficient to maintain resistance to tumor necrosis factor-related apoptosis-inducing ligand-mediated apoptosis in prostate cancer. Cancer Res 2004;64:7086.
9. Poulaki V, Mitsiades CS, Kotoula V, et al. Regulation of Apo2L/tumor necrosis factor-related apoptosis-inducing ligand-induced apoptosis in thyroid carcinoma cells. Am J Pathol 2002;161:643.
10. Nam SY, Jung GA, Hur GC, et al. Upregulation of FLIP(S) by Akt, a possible inhibition mechanism of TRAIL-induced apoptosis in human gastric cancers. Cancer Sci 2003;94:1066.
11. Summerton J, Stein D, Huang SB, et al. Morpholino and phosphorothioate antisense oligomers compared in cell-free and in-cell systems. Antisense Nucleic Acid Drug Dev 1997;7:63.
12. Giles RV, Spiller DG, Clark RE, et al. Antisense morpholino oligonucleotide analog induces mis-splicing of C-myc mRNA. Antisense Nucleic Acid Drug Dev 1999;9:213.
13. Ghosh C, Stein D, Weller D, et al. Evaluation of antisense mechanisms of action. Methods Enzymol 2000;313:135.
14. Iversen PL, Arora V, Acker AJ, et al. Efficacy of antisense morpholino oligomer targeted to c-myc in prostate cancer xenograft murine model and a Phase I safety study in humans. Clin Cancer Res 2003;9:2510.
15. Nikolovska-Coleska Z, Xu L, Hu Z, et al. Discovery of embelin as a cell-permeable, small-molecular weight inhibitor of XIAP through structure-based computational screening of a traditional herbal medicine three-dimensional structure database. J Med Chem 2004;47:2430.
16. Holcik M, Gibson H, Korneluk RG. XIAP: Apoptotic brake and promising therapeutic target. Apoptosis 2001;6:253.
17. Irmler M, Thome M, Hahne M, et al. Inhibition of death receptor signals by cellular FLIP. Nature 1997;388:190.
18. Kinoshita H, Yoshikawa H, Shiiki K, et al. Cisplatin (CDDP) sensitizes human osteosarcoma cell to Fas/CD95-mediated apoptosis by down-regulating FLIP-L expression. Int J Cancer 2000;88:986.
19. Vignati S, Codegoni A, Polato F, et al. TRAIL activity in human ovarian cancer cells: Potentiation of the action of cytotoxic drugs. Eur J Cancer 2002;38:177.
20. Wajant H. Targeting the FLICE inhibitory protein (FLIP) in cancer therapy. Mol Interv 2003;3:124.
21. Xiao CW, Yan X, Li Y, et al. Resistance of human ovarian cancer cells to tumor necrosis factor alpha is a consequence of nuclear factor kappa B-mediated induction of Fas-associated death domain-like interleukin-1beta-converting enzyme-like inhibitory protein. Endocrinology 2003;144:623.

World J Surg (2008) 32:271–278
DOI 10.1007/s00268-007-9281-2

World Journal of Surgery

Intraductal Papillary Mucinous Neoplasms of the Pancreas: Clinicopathologic Characteristics and Long-Term Follow-Up After Resection

Kazuyuki Nagai · Ryuichiro Doi · Atsushi Kida · Kazuhiro Kami · Yoshiya Kawaguchi · Tatsuo Ito · Takaki Sakurai · Shinji Uemoto

Published online: 20 November 2007

Abstract
Background Resection is recommended for main duct intraductal papillary mucinous neoplasms (IPMNs) of the pancreas because of the high risk of malignancy, but the indications for resection of branch duct and mixed-type IPMNs remain controversial. Our objective was to determine the appropriate management of IPMNs based on clinicopathologic characteristics and survival data obtained after resection.
Methods A total of 72 consecutive IPMN patients who underwent resection between January 1984 and June 2006 were reviewed. The lesions were classified as main duct, branch duct, or mixed-type IPMNs and histologically graded as noninvasive (adenoma, borderline neoplasm, carcinoma in situ) or invasive.
Results Main duct IPMNs ($n = 15$) were associated with a significantly worse prognosis than other subtypes. For branch duct ($n = 49$) and mixed-type IPMNs ($n = 8$), the diameter of the cystic lesions was an independent predictor of malignancy by multivariate analysis. However, four patients with cysts <30 mm in diameter and no mural nodules had a malignancy. No patient with noninvasive IPMN died of this disease, showing excellent survival, whereas the 5-year survival rate of patients with invasive IPMNs was only 57.6% and was significantly worse than that of patients with noninvasive IPMNs ($p = 0.0002$).
Conclusions Resection of all main duct IPMNs seems to be reasonable. Invasive IPMNs were associated with significantly worse survival than noninvasive IPMNs. Although the diameter of cystic lesions was a predictor of malignancy for branch duct and mixed-type IPMNs, precise preoperative identification of malignancy was difficult. Therefore, these lesions should be managed by aggressive resection before invasion occurs to improve survival.

K. Nagai · R. Doi (✉) · A. Kida · K. Kami · Y. Kawaguchi · T. Ito · S. Uemoto
Division of Hepato-Biliary-Pancreatic Surgery and Transplantation, Department of Surgery, Kyoto University, 54 Shogoinkawaracho, Sakyo, Kyoto 606-8507, Japan
e-mail: doir@kuhp.kyoto-u.ac.jp

T. Sakurai
Department of Diagnostic Pathology, Kyoto University, Kyoto, Japan

Intraductal papillary mucinous neoplasms (IPMNs) are intraductal mucin-producing neoplasms of the pancreas that cause cystic dilatation of the main and/or branch pancreatic ducts. This neoplasm was first described in 1982 by Ohashi et al. [1] as a mucin-producing tumor of the pancreas; and it was eventually recognized and defined clearly by the World Health Organization (WHO) in 1996 as an intraductal papillary mucinous tumor (IPMT) [2]. In the revised WHO classification published in 2000, IPMT was renamed IPMN [3]. Although IPMNs have been increasingly detected over the last decade, the natural history of this neoplasm is not fully understood, and its management remains controversial [4, 5].

IPMNs are thought to have malignant potential and to undergo transformation from adenoma to borderline neoplasms, followed by carcinoma in situ (CIS), and finally invasive carcinoma, which is the classic adenoma–carcinoma sequence [4]. Complete resection of noninvasive IPMNs (CIS or earlier disease) has been reported to achieve excellent survival [6–8]. On the other hand, the survival rate after resection of invasive IPMNs has been

reported to be markedly worse than that of patients without invasive components [6–8]. Although it is also unclear whether there is a difference of survival between invasive IPMN and pancreatic ductal carcinoma [7, 8], there is general consensus that IPMNs with CIS or invasive carcinoma are potentially fatal diseases unless they are surgically resected [4].

IPMNs can be divided into three subtypes—main duct, branch duct, mixed type—based on imaging findings and/or histology [4, 5]. The frequency of malignancy and the survival rate after resection show differences that depend on the neoplasm subtype. Main duct IPMNs are usually malignant, with the malignancy rate ranging from 60% to 83% [6, 9–11], whereas branch duct IPMNs have a relatively lower frequency of malignancy (6–46%) [6, 9, 10].

The international consensus guidelines [5] recommend resection of all main duct IPMNs if the patient is a good surgical candidate because of the high frequency of malignancy. However, the indications for resection of branch duct IPMNs remain controversial because preoperative identification of malignancy is often difficult. Mixed-type IPMNs are thought to be an advanced form of branch duct IPMNs, but this subtype has not yet been clearly defined [4, 5]. Many of the previous studies on IPMNs were performed without properly defining or classifying these neoplasms. In addition, one pitfall in the classification is that many of the branch duct IPMNs have some degree of involvement in the main duct, as seen by histologic examinations, resulting in many branch duct IPMNs being diagnosed preoperatively as in the mixed category. In practice, therefore, the clinical classification should be done morphologically based on preoperative imaging findings [4].

Factors that predicted malignancy of IPMNs in previous studies were main duct type [12–15], main pancreatic duct dilatation, mural nodules, tumor size [10, 12, 14, 15], dilated papilla of Vater leaking mucin [15], symptoms [14, 15], jaundice [13], and diabetes [12]. With respect to morphologic features, Matsumoto et al. [9] reported that IPMNs with a diameter <30 mm and/or without mural nodules were all benign. Similarly, Sugiyama et al. [10] found that a tumor >30 mm and/or the presence of mural nodules were significant predictors of malignancy by multivariate analysis.

The aim of the present study was to define the clinicopathologic characteristics, imaging findings, and long-term outcome of patients with IPMNs who underwent resection at our institution. Another purpose was to determine the factors correlated with malignancy, which included CIS and invasive carcinoma of the branch duct and mixed-type IPMNs, that we could utilize to determne the indications for surgical resection of these neoplasms.

Patients and methods

A total of 72 consecutive patients with IPMNs who underwent surgical resection between January 1984 and May 2006 at Kyoto University Hospital were reviewed. The diagnosis of IPMN was confirmed histologically by at least two pathologists who examined the resected tissues. IPMNs were distinguished from mucinous cystic neoplasms (MCNs) by the absence of the ovarian-type stroma that is characteristic of the latter neoplasms and by the various well known clinical features [5].

Based on preoperative imaging findings, the IPMNs were classified into three morphologic subtypes: main duct IPMNs, branch duct IPMNs and mixed-type IPMNs. Lesions that predominantly involved the main duct were classified as main duct IPMNs, and lesions that involved a branch duct were classified as branch duct IPMNs. Lesions with involvement of not only a branch duct but also the main duct, with the former being predominantly affected, were classified as mixed-type IPMNs.

The lesions were histologically graded as adenoma, borderline neoplasm, CIS, or invasive carcinoma according to the WHO classification of IPMNs [3]. The first three categories were defined as noninvasive IPMNs. Survival between patients with noninvasive IPMNs and those with invasive IPMNs were compared. Survival between patients with invasive IPMNs and patients with pancreatic ductal carcinomas matched for the UICC stage [16] and the surgical era were also compared.

The clinical characteristics studied were the demographic data, the location of the neoplasm, and presenting symptoms (jaundice, abdominal pain, back pain, fever, loss of weight, a history of pancreatitis, onset or worsening of diabetes). The surgical procedure, postoperative complications, morbidity, and mortality were also investigated. Follow-up information was obtained from medical records or by direct contact with patients or their referring physicians.

Patients with neoplasms located in the head, neck, or uncinate process of the pancreas usually underwent pylorus-preserving pancreatoduodenectomy (PPPD) or pancreatoduodenectomy (PD), whereas patients with neoplasms in the body and/or tail of the pancreas underwent distal pancreatectomy (including spleen-preserving resection). Total pancreatectomy was performed for main duct IPMNs with diffuse involvement or for multiple branch duct IPMNs. Partial resection or middle segmental pancreatectomy was performed in the patients with small branch duct lesions. Peripancreatic lymph nodes were dissected in all patients. In the patients with suspected lymph node metastasis or invasive IPMN diagnosed preoperatively or intraoperatively, extended lymph node dissection was performed with the aim of eradicating residual cancer cells. Intraoperative frozen section examination of the pancreatic

surgical margins was performed routinely. The margin was defined as positive if the duct epithelium showed moderate dysplasia or more advanced changes. In the patients with positive margins, additional resection was continued until a negative result was obtained.

The analysis of the patients with branch duct and mixed-type IPMNs was done to determine the clinical factors correlated with malignancy and thus define the indications for resection. Because mixed-type IPMN is thought to represent an advanced form of branch duct IPMNs [4, 5], branch duct and mixed lesions were combined as branch duct-mixed IPMNs in this analysis. The branch duct-mixed IPMNs were classified as benign (adenoma and borderline neoplasm) or malignant (CIS and invasive carcinoma), and their characteristics were compared to identify predictors of malignancy.

In addition to the above-mentioned clinical characteristics, the following factors were investigated: duration of symptoms, history of alcohol intake and smoking, serum levels of carcinoembryonic antigen (CEA) and carbohydrate antigen 19-9 (CA19-9), imaging findings (including the factors mentioned below), and pancreatic juice cytology. Imaging findings—including the diameter of cystic lesions, the diameter of the main pancreatic duct (MPD), the presence of mural nodules, and mucin secretion from a dilated papilla of Vater—were determined by a combination of abdominal ultrasonography (US), computed tomography (CT), endoscopic retrograde cholangiopancreatography (ERCP), magnetic resonance cholangiopancreatography (MRCP), and endoscopic ultrasonography (EUS). When [^{18}F] fluorodeoxyglucose (FDG)-positron emission tomography (PET) was performed, FDG uptake was quantified; a standardized uptake value (SUV) > 2.2 was defined as indicating accumulation of the tracer [17]. Pancreatic juice for cytology was obtained during ERCP.

Statistical analysis

Continuous variables are presented as the median and range. Comparison between groups was performed by the Mann-Whitney U-test, and categorical variables were compared by the χ^2 test. Multivariate logistic regression analysis was also performed. Survival curves were drawn by the Kaplan-Meier method and were compared by the log-rank test. For all analyses, $p < 0.05$ was considered statistically significant.

Results

Clinical and histologic characteristics

Clinical and histologic characteristics of the 72 patients with IPMN are shown in Table 1. Fifteen patients had main duct IPMNs, 49 patients had branch duct IPMNs, and 8 patients had mixed-type IPMNs. In total, all of the main duct IPMNs were malignant, and 10 of these patients had invasive carcinoma; 29 patients with branch duct and mixed-type IPMNs were malignant, including invasive carcinoma in 18 patients with branch duct IPMNs and 2 patients with mixed-type IPMNs.

Table 1 Clinical and histologic characteristics of 72 patients with IPMN

Parameter	Total ($n = 72$)	Main duct type ($n = 15$)	Branch duct type ($n = 49$)	Mixed type ($n = 8$)
Age (range)	63 (31–85)	64 (31–77)	62 (41–85)	72 (63–75)
Sex (M:F)	44:28	12:3	27:22	5:3
Symptoms	41 (57%)	10	26	5
Jaundice	6 (8%)	1	4	1
Abdominal pain	18 (25%)	5	12	1
Back pain	7 (10%)	3	4	0
Fever	5 (7%)	3	1	1
Body weight loss	16 (22%)	5	9	2
Pancreatitis	9 (13%)	4	4	1
Diabetes	21 (29%)	6	10	5
Neoplasm localization (Ph/Pbt/Phbt)	40/23/9	6/3/6	32/16/1	2/4/2
Histology				
Adenoma	18 (25%)	0	15	3
Borderline	10 (14%)	0	9	1
CIS	14 (19%)	5	7	2
Invasive carcinoma	30 (42%)	10	18	2

IPMN: intraductal papillary mucinous neoplasm; Ph: pancreas head; Pbt: pancreas body and/or tail; Phbt: pancreas head, body, and tail; CIS: carcinoma in situ

Operative procedures and postoperative complications

In terms of the operations done, PPPD was performed in 29 patients, and the other procedures were PD in 8 patients, distal pancreatectomy in 20 patients (including one patient with spleen-preserving distal pancreatectomy), total pancreatectomy in 10 patients, partial resection of the pancreas in 4 patients, and middle segmental pancreatectomy in 1 patient.

The postoperative morbidity rate was 25%, but there were no severe complications that needed further surgical intervention or intensive care (Table 2). There were no deaths related to surgery in this series.

Survival rate and recurrence rate

The mean postoperative follow-up period was 54 months (range 1–267 months). The overall survival rate of patients with main duct IPMNs was significantly lower than that of those with other subtypes (Fig. 1). The overall 5-year and 10-year survival rates of patients with main duct IPMN were 66.7% and 17.8%, respectively. Patients with noninvasive main duct IPMNs ($n = 5$) did not suffer from recurrence and did not die of pancreatic disease, but two patients died of other diseases at more than 5 years after resection (one patient died of esophageal cancer at 62 months after resection, and the other died of liver cirrhosis at 117 months. On the other hand, 6 of 10 patients with invasive main duct IPMNs died of recurrence, including one patient with liver metastasis at the initial operation; another patient died of some other disease (pneumonia at 110 months). Recurrence was local in three patients, and the bone and peritoneum were involved in one patient each.

Table 2 Postoperative complications for 72 patients with IPMN

Complication	No.
Mortality	0
Overall complications	18 (25%)
GI anastomotic leakage	1 (1%)
Pancreatic fistula	4 (6%)
Intraabdominal abscess	1 (1%)
Pancreatitis	1 (1%)
Pancreatic pseudocyst	2 (3%)
Anastomotic stenosis	2 (3%)
Cholangitis	2 (3%)
Delayed gastric emptying	3 (4%)
Ascites	1 (1%)
Diarrhea	2 (3%)
Pneumonia	2 (3%)

GI: gastrointestinal

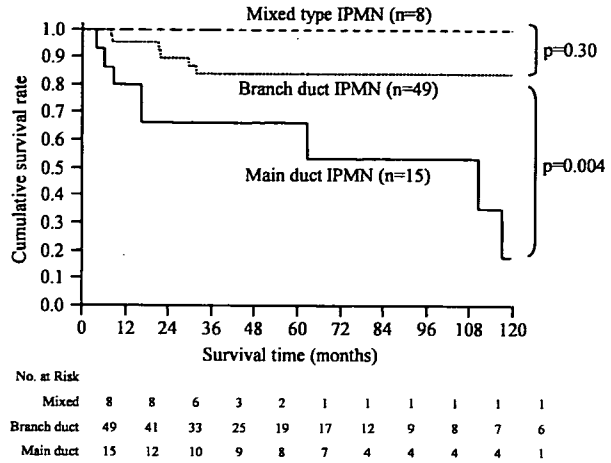

Fig. 1 Overall survival of patients with main duct ($n = 15$), branch duct ($n = 49$), and mixed-type ($n = 8$) intraductal papillary mucinous neoplasms (IPMNs). The 5-year survival rates for main duct, branch duct, and mixed-type IPMNs were 66.7%, 83.6%, and 100%, respectively. The survival of patients with main duct IPMNs was significantly worse than that of the other patients

The 5-year overall survival rate of patients with invasive branch duct-mixed IPMNs ($n = 20$) was 58.4%, which was significantly lower than that of patients with noninvasive branch duct/mixed-type IPMNs ($p = 0.0003$) (Fig. 2). None of the patients with noninvasive branch duct/mixed-type IPMNs ($n = 37$) had recurrence, and their 10-year overall survival rate was 100%. In contrast, six patients with invasive branch duct/mixed-type IPMN died, with the cause of death being recurrence in four patients (local recurrence in two patients, peritoneal dissemination in one patient, and unknown in one patient) and other diseases in two patients (unknown disease in one patient and bile duct

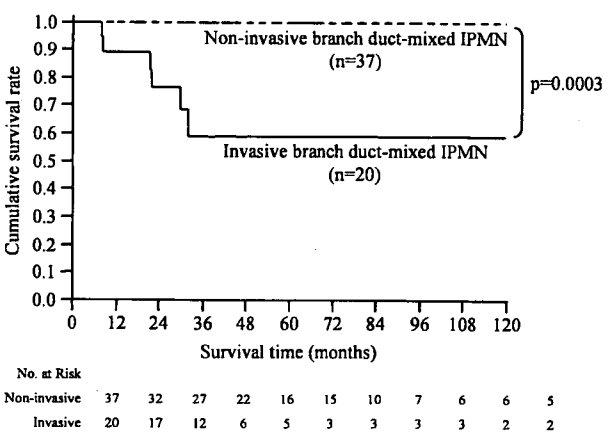

Fig. 2 Overall survival of patients with invasive branch duct/mixed-type IPMNs ($n = 37$) and noninvasive IPMNs ($n = 20$). The overall survival rate of patients with branch duct/mixed-type IPMNs was significantly lower than that of patients with noninvasive IPMNs ($p = 0.0003$). No patient from the latter group died

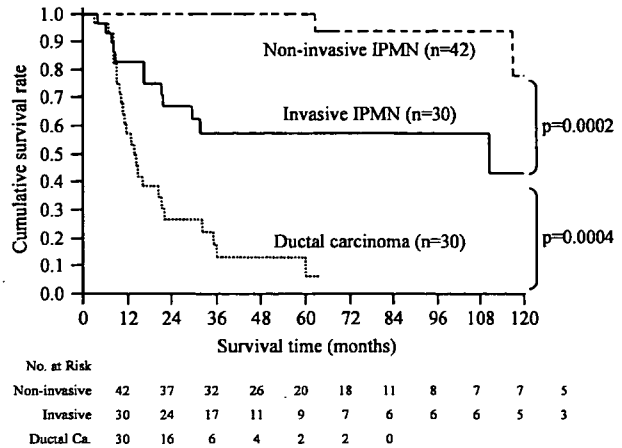

Fig. 3 Overall survival of patients with invasive IPMNs ($n = 30$), noninvasive IPMNs ($n = 42$), and pancreatic ductal carcinoma ($n = 30$) matched for tumor stage and surgical era. The survival rate of patients with noninvasive IPMNs was excellent. The 5-year survival rate of patients with invasive IPMNs was 57.6%, which was significantly lower than that of patients with noninvasive IPMNs ($p = 0.0002$) but better than that of matched patients with pancreatic ductal carcinoma ($p = 0.0004$)

carcinoma in one patient). Two other patients with local recurrence are alive at 30 months and 39 months after surgery, respectively.

A comparison between invasive and noninvasive IPMNs of all subtypes is shown in Figure 3. The survival rate of patients with noninvasive IPMNs ($n = 42$) was excellent, and the overall 5- and 10-year survival rates were 100% and 78.1%, respectively. In contrast, the overall 5- and 10-year survival rates of patients with invasive IPMNs ($n = 30$) were 57.6% and 43.2%, respectively, which were significantly lower than those for noninvasive IPMNs ($p = 0.0002$) but higher than those of matched patients with ductal carcinoma ($p = 0.0004$).

Clinical predictors of malignancy for branch duct and mixed-type IPMNs

A total of 49 patients with branch duct IPMNs and 8 patients with mixed-type IPMNs were combined into a single group of branch duct-mixed IPMNs. These 57 patients comprised 28 with benign neoplasms and 29 with malignant neoplasms. The clinical characteristics of the benign and malignant groups are compared in Table 3.

There were no significant differences of age and sex between the benign and malignant groups. Six clinical factors—abdominal pain, weight loss, serum CA19-9 levels, MPD diameter, diameter of cystic lesions, presence of mural nodules—showed a significant correlation with malignancy by univariate analysis (Table 3). The mean duration of symptoms was not different between the two groups, and habitual alcohol intake and a history of smoking were generally similar in the two groups.

Serum CEA and CA19-9 levels were measured in 40 patients (18 in the benign group, 22 in the malignant group) and 49 patients (24 in the benign group, 25 in the malignant), respectively. All patients underwent transabdominal US. CT was done in 56 patients, and the other imaging modalities were ERCP in 52 patients, MRCP in 40 patients, and EUS in 45 patients. The presence or absence of mucin and a dilated papilla of Vater were determined in 38 and 37 patients, respectively, by ERCP and/or duodenoscopy. Pancreatic juice cytology was investigated in 19 patients and FDG-PET was performed in 28 patients.

CA19-9 levels, which had a significant correlation with malignancy by univariate analysis, showed a wide range in the malignant group and exceeded 100 U/ml in seven patients, wheeas only one patient from the benign group had such a high level.

Mucin and dilation of the papilla of Vater were observed in about 40% of the patients even in the benign group. The specificity and sensitivity of pancreatic juice cytology for the malignant group were 90% and 44%, respectively. The specificity and sensitivity of FDG-PET for malignant group were 57% and 64%, respectively.

When multivariate analysis of the above factors was performed, the diameter of cystic lesions was the only independent predictor of malignancy that was identified (Table 4).

The relation between the diameter of cystic lesions and the presence of mural nodules was further investigated in the benign and malignant groups (Fig. 4). Although the presence of mural nodules was correlated with malignancy by univariate analysis (Table 3) and the diameter of cystic lesions was the only independent predictor on multivariate analysis (Table 4), 10 patients from the benign group had mural nodules and 4 patients who had cystic lesions <30 mm in diameter and no mural nodules were found to have malignant IPMNs (including three patients with CIS and one patient with invasive carcinoma). Moreover, two of these patients were asymptomatic.

Discussion

Since the first report by Ohashi et al. [1] in 1982, IPMNs have been recognized with increasing frequency. This neoplasm features a broad spectrum of histologic abnormalities that range from adenoma to invasive carcinoma [4]. The only definitive treatment for IPMNs is surgical resection, and complete resection of noninvasive IPMNs (adenoma, borderline neoplasms, CIS) achieves an excellent survival rate [6–8]. On the other hand, the survival rate of patients with invasive IPMNs is significantly lower than

Table 3 Comparison of the clinical characteristics and laboratory and imaging findings of branch duct and mixed-type IPMNs between the benign and the malignant groups by univariate analysis

Parameter	Benign (n = 28)	Malignant (n = 29)	p
Sex (M:F)	13:15	19:10	0.147
Age (range)	63 (46–80)	64 (41–85)	0.823
Symptoms	13	18	0.235
Jaundice	1	4	0.173
Abdominal pain	3	10	**0.033**
Back pain	1	3	0.317
Fever	0	2	0.199
Loss of body weight	1	10	**0.003**
History of pancreatitis	2	3	0.669
Onset or worsening of diabetes	9	6	0.326
Duration of symptoms (months)	11 (0–144)	2 (1–216)	0.973
History of smoking	15	17	0.701
Habit of alcohol drinking	12	11	0.705
CEA (ng/ml)	1.4 (0–7.3)	1.2 (0–6.9)	0.932
CA19-9 (U/ml)	13.0 (4.0–694.0)	27.2 (2.0–1555.0)	**0.035**
MPD diameter (mm)	2.0 (1.0–13.0)	5.0 (2.0–20.0)	**0.005**
Cystic lesions diameter (mm)	23.5 (5.0–43.0)	35.0 (15.0–90.0)	**0.0002**
Presence of mural nodule	10	20	**0.012**
Mucin secretion (yes:no)	7:12	12:7	0.141
Dilated orifice of papilla (yes:no)	8:11	11:7	0.248
Cytology (positive:negative)	1:9	4:5	0.088
FDG uptake (positive:negative)	5:9	8:6	0.256

MPD: main pancreatic duct; FDG: [^{18}F]fluorodeoxyglucose

The p values in boldface indicate significance

that of patients without invasive cancer. However, there is no current consensus as to whether invasive IPMNs have a poor prognosis similar to that of pancreatic ductal carcinomas. In our series, 42 patients with noninvasive IPMNs did not suffer from recurrence or die of their disease after resection and showed excellent survival. In contrast, the 5-year survival rate of patients with invasive IPMNs was only 57.6%, which was significantly lower than that of patients with noninvasive IPMNs (p = 0.0002), although it was better than that of ductal carcinoma patients matched for the UICC stage [16] and the surgical era.

IPMNs are classified as main duct, branch duct, and mixed-type IPMNs [4, 5]. Because there are significant differences in the frequency of malignancy and other clinical characteristics between main duct and branch duct IPMNs, these two types should be distinguished preoperatively based on imaging findings to allow appropriate clinical management. However, there are still some ambiguities related to this morphologic classification [4, 5]. In many previous studies of IPMNs, analyses were done without proper definition or classification of the neoplasms.

Table 4 Results of the multivariate analysis for clinical characteristics and laboratory and imaging findings in benign and malignant branch duct and mixed-type IPMNs

Parameter	Odds ratio (95% CI)	p
Cystic lesion diameter (mm)	940.02 (9.95–621915.38)	0.012
Body weight loss	8.93 (0.98–211.71)	0.085
Mural nodules	2.69 (0.68–11.55)	0.165
MPD diameter (mm)	7.79 (0.26–313.61)	0.251
Abdominal pain	1.26 (0.19–8.43)	0.804
CA19-9 (U/ml)	3.54 (0.0003–93,458.61)	0.835

CI: confidence interval; MPD: main pancreatic duct

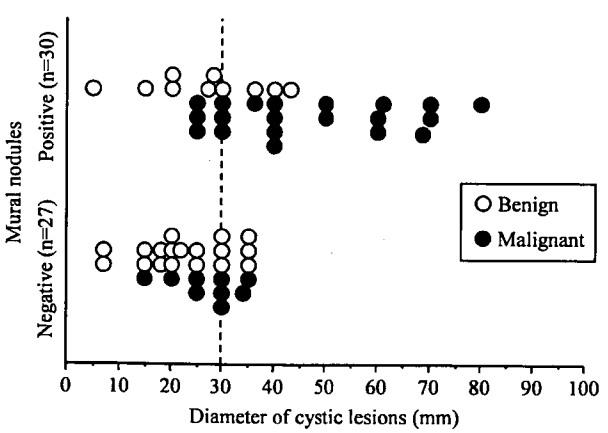

Fig. 4 Relation between the diameter of cystic lesions and the presence of mural nodules in patients with benign or malignant branch duct-mixed IPMNs. Ten patients in the benign group had mural nodules. Note that four patients with cystic lesions <30 mm diameter and without mural nodules had malignant neoplasms

In this study, all of the neoplasms were preoperatively classified according to the above-mentioned definitions.

There is general agreement that main duct IPMNs should be resected if the patient is a suitable candidate for surgery because of the high risk of malignancy [5]. In our series, all of the main duct IPMNs were malignant, and these patients had a significantly lower survival rate than those with other subtypes. Although the patients with main duct IPMNs comprised 21% of our series, similar to the percentage reported in the previous studies [7, 10, 18], the reason for the high malignancy rate associated with main duct IPMNs is unknown. However, resection of main duct IPMNs seems to be a reasonable approach to treatment.

The indications for resection of branch duct and mixed-type IPMNs remain controversial because malignancy is less common than in main duct IPMNs and the preoperative detection of malignancy is often difficult. Therefore, we focused on identifying factors that could be used to predict malignancy of branch duct and mixed-type IPMNs. As a result, we identified abdominal pain, weight loss, serum CA19-9 levels, MPD diameter, the diameter of cystic lesions, and the presence of mural nodules as factors significantly associated with malignancy on univariate analysis. However, the diameter of cystic lesions was the only independent predictor of malignancy on multivariate analysis. Other factors, such as a tumor marker (CEA), mucin leaking from a dilated papilla, pancreatic juice cytology, and accumulation on FDG-PET, showed no significance as predictors of malignancy.

Preoperative evaluation of IPMNs by various imaging modalities (e.g., US, CT, EUS, ERCP, MRCP) is essential before making a decision about treatment. EUS has been reported to be the most useful modality for detecting mural nodules, with an accuracy of 92.3%–100% [14, 19]. However, demonstration of mural nodules is often difficult even with EUS, and one reason may be the difficulty of differentiating nodules from mucin plugs. Another problem is that the diagnostic accuracy of EUS depends on the operator's technique and experience. On the other hand, the diameter of cystic lesions (the only independent predictor of malignancy in our multivariate analysis) can be objectively determined by EUS or other conventional imaging modalities such as abdominal US and CT. Therefore, determining the malignancy of branch duct and mixed-type IPMNs based on the diameter of cystic lesions may be a practical approach.

In the international guidelines [5], positive symptoms and cysts >30 mm in size are described as important for predicting the malignancy of branch duct IPMNs. Matsumoto et al. [9] and Sugiyama et al. [10] reported that a tumor <30 mm and the absence of mural nodules suggested benign disease in patients with branch duct IPMNs. Therefore, the guidelines [5] state that asymptomatic patients with small branch duct IPMNs may be managed by careful follow-up. However, our series of 57 patients with branch duct and mixed-type IPMNs included four patients who had cystic lesions <30 mm in diameter without mural nodules that were malignant, and two of these patients were asymptomatic.

These results indicate that predicting malignancy based on symptoms, mural nodules, and the cysts diameter is generally correct although not always accurate. In other words, we have to keep in mind that none of these factors can precisely predict malignancy.

It is quite important for surgical resection, which is the only curative treatment for IPMNs, to achieve excellent survival before the neoplasm becomes invasive [6–8]. It should be emphasized that pancreatic resection has now become a feasible procedure that is performed safely at hospitals with a sufficient case load [20, 21]. In our series, there were no deaths and no severe complications after surgery.

Conclusions

Our conclusion about the surgical indications for branch duct and mixed type IPMNs is as follows: Given the difficulty of predicting malignancy and the unsatisfactory survival of patients with invasive components, these lesions should be managed by aggressive resection at high-volume hospitals before invasion occurs. This strategy should result in improved survival of patients with IPMNs. Of course, all clinical management should be decided by taking into consideration the patient's wishes and after obtaining informed consent.

Acknowledgments This work was supported by Grants-in-Aid (17390364, 17659409) from the Ministry of Education, Culture, Sports, Science, and Technology of Japan.

References

1. Ohashi K, Murakami Y, Maruyama M, et al. (1982) Four cases of "mucin-producing" cancer of the pancreas on specific findings of the papilla of Vater [in Japanese]. Prog Dig Endosc 20:348–351
2. Kloeppel G, Solcia E, Longnecker DS, et al. (1996) Histological typing of tumours of the exocrine pancreas. in: World Health Organization International Histological Classification of Tumours. 2nd edition. Springer, Berlin
3. Longnecker DS, Adler G, Hruban RH, et al. (2000) Intraductal papillary mucinous neoplasms of the pancreas. In: Hamilton SR, Aaltonen LA (eds) World Health Organization Classification of Tumours, Pathology and Genetics of Tumors of the Digestive System. IARC Press, Lyon, pp 237–241
4. Tanaka M, Kiishiro K, Kazuhiro M, et al. (2005) Clinical aspects of intraductal papillary mucinous neoplasm of the pancreas. J Gastroenterol 40:669–675

5. Tanaka M, Chari S, Adsay V, et al. (2006) International consensus guidelines for management of intraductal papillary mucinous neoplasm and mucinous cystic neoplasm of the pancreas. Pancreatology 6:17–32
6. Doi R, Fujimoto K, Wada M, et al. (2002) Surgical management of intraductal papillary mucinous tumor of the pancreas. Surgery 132:80–85
7. Sohn TA, Yeo CJ, Cameron JL, et al. (2004) Intraductal papillary mucinous neoplasms of the pancreas: an updated experience. Ann Surg 239:788–799
8. Wada K, Kozarek RA, Traverso LW (2005) Outcomes following resection of invasive and noninvasive intraductal papillary mucinous neoplasms of the pancreas. Am J Surg 189:632–637
9. Matsumoto T, Aramaki M, Yada K, et al. (2003) Optimal management of the branch duct type intraductal papillary mucinous neoplasms of the pancreas. J Clin Gastroenterol 36:261–265
10. Sugiyama M, Izumisato Y, Abe N, et al. (2003) Predictive factors for malignancy in intraductal papillary mucinous tumours of the pancreas. Br J Surg 90:1244–1249
11. Salvia R, Fernández-del Castillo C, Bassi C, et al. (2004) Main-duct intraductal papillary mucinous neoplasms of the pancreas: clinical predictors of malignancy and long-term survival following resection. Ann Surg 239:678–687
12. Yamaguchi K, Ogawa Y, Chijiiwa K, et al. (1996) Mucin hypersecreting tumors of the pancreas: assessing the grade of malignancy preoperatively. Am J Surg 171:427–431
13. Traverso LW, Peralta EA, Ryan JA Jr, et al. (1998) Intraductal neoplasms of the pancreas. Am J Surg 175:426–432
14. Sugiyama M, Atomi Y (1998) Intraductal papillary mucinous tumors of the pancreas: imaging studies and treatment strategies. Ann Surg 228:685–691
15. Shima Y, Mori M, Takakura N, et al. (2000) Diagnosis and management of cystic pancreatic tumours with mucin production. Br J Surg 87:1041–1047
16. Sobin LH, Wittekind Ch (2002) International Union Against Cancer (UICC): TNM Classification of Malignant Tumours. 6th edition. Wiley-Liss, New York
17. Inokuma T, Tamaki N, Torizuka T, et al. (1995) Eevaluation of pancreatic tumors with positron emission tomography and ^{18}F-fluorodeoxyglucose: comparison with CT and US. Radiology 195:345–352
18. Suzuki Y, Atomi Y, Sugiyama M, et al. (2004) Cystic neoplasms of the pancreas: a Japanese multiinstitutional study of intraductal papillary mucinous tumor and mucinous cystic tumor. Pancreas 28:241–246
19. Yamao K, Ohashi K, Nakamura T, et al. (2001) Evaluation of various imaging methods in the differential diagnosis of intraductal papillary mucinous tumor (IPMT) of the pancreas. Hepatogastroenterology 48:962–966
20. Sosa JA, Bowman HM, Gordon TA, et al. (1998) Importance of hospital volume in the overall management of pancreatic cancer. Ann Surg 228:429–438
21. Gouma DJ, van Geenen RC, van Gulik TM, et al. (2000) Rates of complications and death after pancreaticoduodenectomy: risk factors and the impact of hospital volume. Ann Surg 232: 786–795

Int. J. Cancer: 120, 1355–1363 (2007)

Involvement of ribonucleotide reductase M1 subunit overexpression in gemcitabine resistance of human pancreatic cancer

Shin Nakahira[1,2], Shoji Nakamori[1,3*], Masanori Tsujie[1], Yuji Takahashi[1], Jiro Okami[1], Shinichi Yoshioka[1], Makoto Yamasaki[1], Shigeru Marubashi[1], Ichiro Takemasa[1], Atsushi Miyamoto[1], Yutaka Takeda[1], Hiroaki Nagano[1], Keizo Dono[1], Koji Umeshita[1], Masato Sakon[1] and Morito Monden[1]

[1]*Department of Surgery and Clinical Oncology, Graduate School of Medicine, Osaka University, Suita, Osaka, Japan*
[2]*Department of Surgery, Kansai Rosai Hospital, Amagasaki, Hyogo, Japan*
[3]*Department of Surgery, Osaka National Hospital, National Hospital Organization, Chuo-ku, Osaka, Japan*

Pancreatic cancer is the most lethal of all solid tumors partially because of its chemoresistance. Although gemcitabine is widely used as a first selected agent for the treatment of this disease despite low response rate, molecular mechanisms of gemcitabine resistance in pancreatic cancer still remain obscure. The aim of this study is to elucidate the mechanisms of gemcitabine resistance. The 81-fold gemcitabine resistant variant MiaPaCa2-RG was selected from pancreatic cancer cell line MiaPaCa2. By microarray analysis between MiaPaCa2 and MiaPaCa2-RG, 43 genes (0.04%) were altered expression of more than 2-fold. The most upregulated gene in MiaPaCa2-RG was ribonucleotide reductase M1 subunit (RRM1) with 4.5-fold up-regulation. Transfection with RRM1-specific RNAi suppressed more than 90% of RRM1 mRNA and protein expression. After RRM1-specific RNAi transfection, gemcitabine chemoresistance of MiaPaCa2-RG was reduced to the same level of MiaPaCa2. The 18 recurrent pancreatic cancer patients treated by gemcitabine were divided into 2 groups by RRM1 levels. There was a significant association between gemcitabine response and RRM1 expression ($p = 0.018$). Patients with high RRM1 levels had poor survival after gemcitabine treatment than those with low RRM1 levels ($p = 0.016$). RRM1 should be a key molecule in gemcitabine resistance in human pancreatic cancer through both *in vitro* and clinical models. RRM1 may have the potential as predictor and modulator of gemcitabine treatment.

Key words: gemcitabine; pancreatic cancer; drug resistance; RRM1; microarray

Pancreatic cancer remains one of the most malignant cancers. Although surgery is the only curative treatment currently available, over 80% of patients have advanced regional disease or distant metastasis at the time of diagnosis and less than 20% of the patients are candidates for resection.[1] Therefore, chemotherapy, radiation or a combination of these therapies most commonly plays an important role in pancreatic cancer treatment. They have not had a significant impact on survival rates in recent decades, however, despite many clinical trials.[1]

Gemcitabine (2′,2′-difluorodeoxycytidine, dFdC, Gemzar) has been recognized as the standard first-line chemotherapeutic agent used in patients with pancreatic cancer, since it was shown to have some meaningful impact on either survival or disease-related symptoms when compared with 5-fluorouracil (5-FU) in randomized trials.[2] However, not more than 25% patients with pancreatic cancer will benefit from gemcitabine, a proportion that is slightly less than in patients with other cancers.[2] Although gemcitabine in combination with other various cytotoxic agents is being investigated, no randomized phase III trial has yet established any survival benefit for combination therapy when compared with gemcitabine alone.[1,3] The major cause of this relative treatment failure is thought to be tumor cell resistance to chemotherapy, whether it is inherent or acquired.[4]

A variety of attempts have recently been undertaken *in vitro* to detect the molecular markers of gemcitabine resistance. Alterations involved in cell cycle regulation, proliferation or apoptosis, such as mutated *p53*,[5] Bcl-xl,[6] c-*Src*,[7] focal adhesion kinase[8] and BNIP3,[9] have been described in a variety of cancers including pancreatic cancer. Nucleotide transporters were also described as molecules related to the intracellular transport of extracellular gemcitabine from outside.[10,11] The ribonucleotide reductase M1 subunit (RRM1),[12,13] ribonucleotide reductase M2 subunit (RRM2),[14,15] deoxycytidine kinase (dCK)[16] and cytidine deaminase (CDA)[17] are supposed to play a role in gemcitabine resistance of the variety of cancer as metabolic enzymes of the drug. However, they remain still controversial because of the lack of direct evidence based on either *in vitro* gene transfer model systems or clinical data from patients with pancreatic cancer.

Variant cells with characteristics resistant to chemotherapeutic agents have widely contributed to the investigation of molecular mechanisms in chemoresistance.[7,12,13,16,18,19] These chemoresistant variants are traditionally established by continuous drug exposure and gradually increased drug concentration. Although drug resistance can occur at many levels, including increased drug efflux, drug inactivation, alterations in drug target, processing of drug-induced damage and evasion of apoptosis,[20] the advent of recently established analytical technologies such as microarray and protein array systems has opened up feasible opportunities to identify molecules involved in drug resistance. Indeed, microarray analysis has become a key tool for characterizing gene expression in a variety of experimental systems with chemoresistant variants and has succeeded in identifying the molecules associated with gemcitabine resistance using an oligonucleotide microarray system *in vitro* and *in vivo*.[12,13,21]

In this study, we developed gemcitabine-resistant cells from the human pancreatic cancer cell lines and attempted to identify novel genes involved in gemcitabine chemoresistance using an oligonucleotide microarray system covering 30,000 human oligonucleotides. Furthermore, the detected candidate gene was also revealed to be responsible for gemcitabine resistance by an RNAi assay and by clinical analysis of the patients treated with gemcitabine.

Material and methods

Pancreatic cancer cell lines and selection of gemcitabine resistant cells

Five types of human pancreatic carcinoma cell lines were used in the present study. MiaPaCa-2 and PSN1 cell lines were obtained from the Japanese Collection of Research Bioresources (JCRB, Tokyo, Japan). The BxPC3 and Panc1 cell lines were obtained from the American Type Culture Collection (ATCC,

Grant sponsors: Ministry of Health, Labour and Welfare, Japan; Society for the Promotion of Science.
*Correspondence to: Department of Surgery, Osaka National Hospital, National Hospital Organization, 2-1-14 Hoenzaka, Chuo-ku, Osaka 540-0006, Japan. Fax: +81-6-6943-6467. E-mail: nakamori@onh.go.jp
Received 7 May 2006; Accepted after revision 29 August 2006
DOI 10.1002/ijc.22390
Published online 27 November 2006 in Wiley InterScience (www.interscience.wiley.com).

Rockville, MD). The PCI6 cell line was a gift from Dr. H. Ishikawa (Hokkaido University, Sapporo, Japan). All cell lines were cultured at 37°C under 5% CO_2 in DMEM (Sigma Chemical Co., St. Louis, MO) supplemented with 10% FBS (Hyclone Laboratories, Inc., Rockville, MD) and 100 units/ml each of penicillin and streptomycin. Relative gemcitabine-sensitive cell lines, BxPC3, PSN1 and MiaPaCa2 were used for the establishment of chemoresistant variants. Gemcitabine-resistant cells were generated by exposure to gradually increasing concentrations of the drug for 2 months as described previously.[12,22] The starting concentration was 1 ng/ml gemcitabine. When cells adapted to the drug, the gemcitabine concentration was increased. The final concentrations were 10 ng/ml gemcitabine for PSN1 and 20 ng/ml gemcitabine for BxPC3 and MiaPaCa-2.

Reagents

Gemcitabine was kindly provided by Eli Lilly Pharmaceuticals (Indianapolis, IN). 5-Fluorouracil (5-FU) was purchased from Sigma Chemical Co. Gemcitabine and 5-FU were dissolved in distilled water and applied to cells at a concentration of less than 0.1% of the medium volume.

Cytotoxicity assay

Cell growth was assessed by the 3-(4-, 5-dimethylthiazol-2-yl)-2, 5-diphenyl tetrazolium bromide (MTT) (Sigma Chemical Co.) method.[23] Briefly, 3×10^4 cells were seeded to a 96-well plate in 100 µl of medium and left overnight to adhere. Several concentrations of the test drugs in 100 µl volumes were added, and the cells were incubated for 48 hr. After treatment, 10 µl of MTT solution (5 mg/ml) was added to each well and incubated for another 4 hr at 37°C. Then, 100 µl of acid-isopropanol was added, and after 24 hr at 4°C, reduced MTT was measured spectrophotomechanically in a dual beam microtiter plate reader at 570 nm with a 650 nm reference. Resulting absorbencies were converted to percent survival by comparing treated with untreated (100% survival) cells. 50% inhibitory concentrations (IC_{50}s) are defined as the concentrations of drug that result in 50% cell survival when compared with untreated cells.

Growth curve

Cells (1×10^4) were seeded to a 24-well plate in 1 ml of medium and left overnight to adhere. The medium was replaced daily with 1 ml of fresh medium with or without gemcitabine at the dose of parental IC_{50}. Cell numbers were counted with an automatic cell counter (Celltec MEK-5103, Nihon Kohden, Tokyo, Japan) after being treated with trypsin.

Animals and in vivo *antitumor experiments*

Four-week-old female BALB/c nu/nu mice were purchased from Japan Clea (Tokyo, Japan) and maintained in specific pathogen-free conditions. Human pancreatic tumor xenografts were prepared by subcutaneous implantation (5×10^6 cells; total volume 100 µl) of MiaPaCa2 and MiaPaCa2-RG, resistant variant established from MiaPaCa2, into the right back of 10 nude mice each. The animals were monitored for activity, physical condition, determination of body weight and measurement of tumor volume [1/2 × (the major axis) × (the minor axis)^2] every other day. When the tumors reached a volume between 100 and 200 mm^3, mice were divided into the following 4 groups of 5 mice each: parental cell with no treatment, parental cell with weekly intraperitoneal injections of gemcitabine, resistant cell with no treatment, resistant cell with weekly intraperitoneal injections of gemcitabine. Gemcitabine was injected weekly into the peritoneal cavity at the dose of 240 mg/kg as described.[24]

[^{3}H] gemcitabine cellular uptake assay

Cells were seeded to a flat-bottomed 24-well microplate (1×10^4/well) and incubated for 24 hr. The medium was replaced by 1 ml of fresh medium by an additional 48 hr of culture. The cells were then exposed to [^{3}H] gemcitabine (Moravek Biochemicals, Inc. Brea, CA) at a concentration of 23.9 ng/ml (1.0 µCi/ml). After 1-hr exposure, the cells were washed 3 times in 1 ml of ice cold phosphate-buffered saline (PBS). The cells were then dissolved in 0.5 ml of 0.5% Triton X-100, and 0.4 ml aliquots were sampled for radioactivity counting. Aliquots of 20 µl were also sampled for protein determination. The uptake level of [^{3}H] gemcitabine was expressed as radioactivity levels divided by protein concentrations measured by the Bradford method (Bio-Rad Laboratories, Hercules, CA).

TABLE I – IC_{50} OF GEMCITABINE (GEM) AND 5-FLUOROURACIL (5-FU) IN GEMCITABINE-SELECTED PANCREATIC CANCER CELL LINES

Cell lines	Drug	IC_{50} (mean ± SD)		Fold resistance
		Parental cell	Resistant cell	
BxPC3	GEM (ng/ml)	50.5 ± 7.1	556.6 ± 76	11-fold
	5-FU (µg/ml)	0.6 ± 0.2	37.5 ± 4.1	60-fold
MiaPaCa2	GEM (ng/ml)	44 ± 5.3	3592.1 ± 170	81-fold
	5-FU (µg/ml)	2.4 ± 0.3	3.07 ± 0.14	1.3-fold
PSN1	GEM (ng/ml)	3.4 ± 0.3	3392 ± 44	986-fold
	5-FU (µg/ml)	1.4 ± 0.1	45 ± 2.6	32-fold

Oligonucleotide microarray

RNA extraction was carried out with TRIzol reagent (Invitrogen, Carlsbad, CA) using a single-step method,[25] and RNA quality was checked with an RNA 6000 Nano LabChip kit (Agilent Technologies, Waldbronn, Germany) according to the manufacturer's protocols. An oligo-microarray covering 30,000 human oligonucleotides (AceGene human 30K; DNA Chip Research Inc. and Hitachi Software Engineering Co., Ltd., Yokohama, Japan) was used in this study.[26] Sample preparation, hybridization and wash were carried out according to the manufacturer's protocols (http://www.dna-chip.co.jp/thesis/AceGeneProtocol.pdf). A sample and the reference were labeled with Cy5-dUTP and Cy3-dUTP (Amersham Pharmacia Biotech, Piscataway, NJ), respectively, mixed, and hybridized on a microarray. The hybridized array was scanned using ScanArray 4000 (GSI Lumonics) at wavelengths corresponding to each probe's unique fluorescence (635 and 532 nm for Cy5 and Cy3, respectively). The signal intensity of each spot (16 bit tiff image) was converted into text format by DNASISArray software (Hitachi software Inc., Tokyo, Japan). Data processing was performed through background subtraction using the average blank spot intensity in each block. If the signal was higher than the background and the signal levels of Cy3 and Cy5 were higher than 1,000, these data were used for further analysis. At this stage, 10,517 genes remained. The Cy3/Cy5 ratio values of each spot were log-transformed and normalized so that the median Cy3/Cy5 ratio of whole genes was 1.0.[27]

Reverse transcription-polymerase chain reaction

RNA extraction was carried out with TRIzol reagent (Invitrogen, Carlsbad, CA), and cDNA was generated with avian myeloblastosis virus reverse transcriptase (Promega, Madison, WI), as described previously.[25] In this assay, porphobilinogen deaminase (PBGD) mRNA was used as an internal control.[28] PCR was performed in a 25-µl reaction mixture containing 2 µl of cDNA template, 1× PerkinElmer PCR buffer, 1.5 mM $MgCl_2$, 0.8 mM deoxynucleotide triphosphates, 0.2 µM each primer and 1 U of Taq DNA polymerase (AmpliTaq Gold, Roche Molecular System, Inc.). The primers for PBGD were synthesized as described previously.[28] The PCR primers used for the detection were as follows: dCK (forward primer, 5′-TGCAGGGAAGTCAACATT-3′; reverse primer, 5′-TCCCACCATTTTTCTGAG-3′), CTP synthetase (forward primer, 5′-CTCATATCACAGATGCAATC-3′; reverse primer, 5′-GATCATATCTGTCAGCCATCTC-3′), CDA (forward primer, 5′-GGAGGCCAAGAAGTCAG-3′; reverse primer, 5′-GACGGCCTTCTGGATAG-3′), DCTD (forward primer, 5′-GTGCAGTGATGACGTGTGTTGC-3′; reverse primer, 5′-CATGTAGATTCCATGTGAC-3′), RRM1 (forward primer, 5′-GAAGACTGGGATGTATTATTTAAG-3′; reverse primer, 5′-CAGAATAACCTATAGGAC-3′), RRM2 (for-

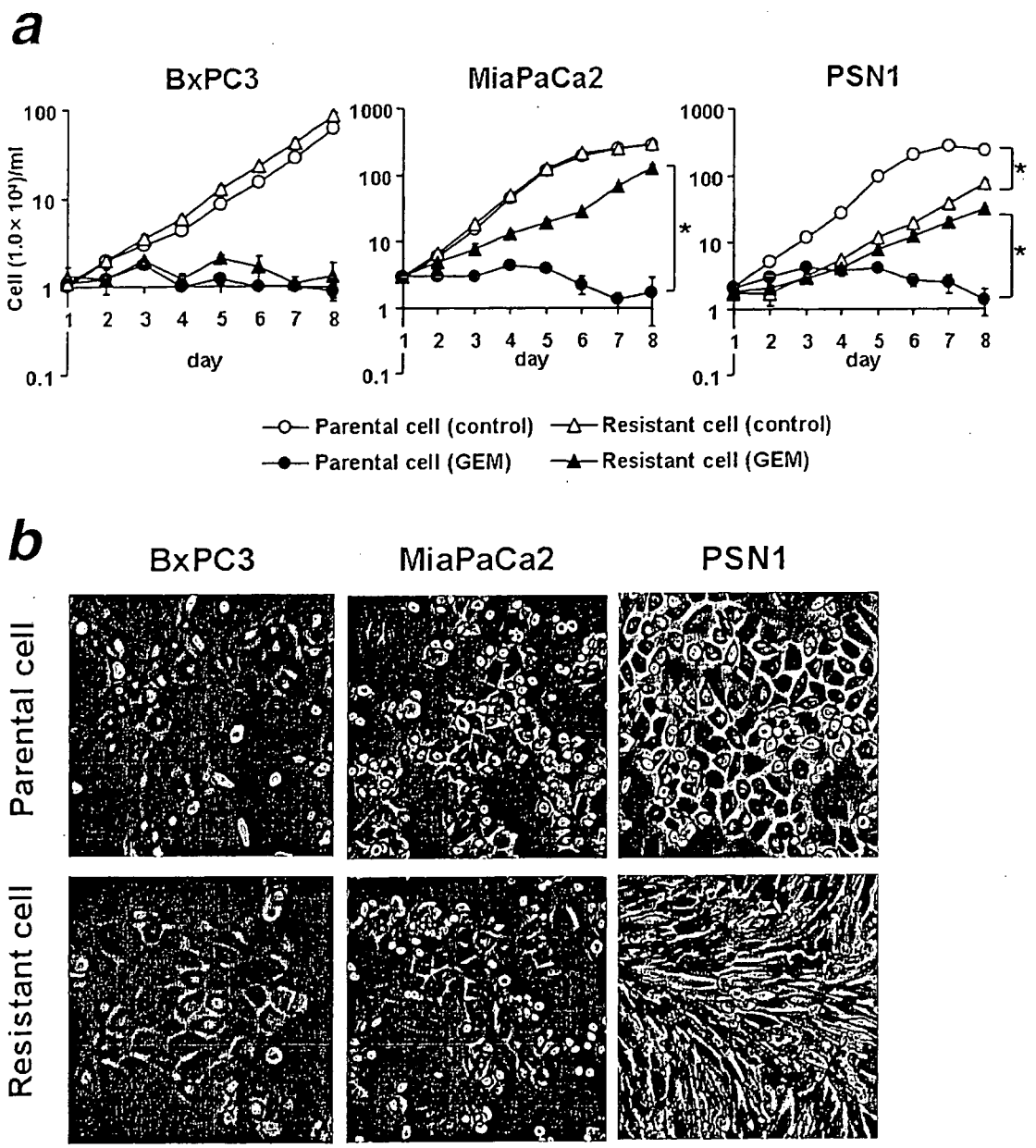

FIGURE 1 – (*a*) Growth curves of pancreatic cancer cell lines. In the absence of gemcitabine (open circle, open triangle) and in continuous exposure to gemcitabine at the dose of parental IC_{50}s (closed circle and closed triangle). Points, mean; bars, SD ($n = 3$). *$p < 0.01$. (*b*) Morphology of pancreatic cancer cell lines, BxPC3, MiaPaCa2, PSN1 and gemcitabine-resistant variants, BxPC3-RG, MiaPaCa2-RG, PSN1-RG. (Original magnification, ×40).

ward primer, 5′-ATGAAAACTTGGTGGAGCGATT-3′; reverse primer, 5′-TGGCAATTTGGAAGCCATAGA-3′), p53R2 (forward primer, 5′-CCAGTTGGCCTCATTGGAAT-3′; reverse primer, 5′-TAGAGTTTTAAAACGAGAGG-3′), ENT1 (forward primer, 5′-GCTTGAAGGACCCGGGGAGC-3′; reverse primer, 5′-TGGAGAAGGCAAAGGCAGCCA-3′). PCR was performed with cycling conditions of 95°C for 10 min, followed by 35 cycles of denaturation at 95°C for 30 sec, annealing at 62°C (RRM1: 57°C) for 30 sec and extension at 72°C for 60 sec, and the products were run on 2% agarose gels and visualized by ethidium bromide staining. A quantitative gene expression assay was performed using LightCycler (Idaho Technology, Salt Lake City, UT), as described previously.[29] PCR was performed with cycling conditions of 95°C for 10 min, followed by 40 cycles of denaturation at 95°C for 10 sec, annealing at 62°C (RRM1: 57°C) for 10 sec and extension at 72°C for 20 sec. Quantification data from each sample were analyzed using the LightCycler analysis software (Roche Diagnostics, Mannheim, Germany) as recommended by the manufacturer. Relative gene expression levels are expressed as quantified gene expression divided by quantified PBGD levels.

Western blotting

Cells grown to subconfluence in 90-mm dishes were lysed in protease inhibitor (1 mM PMSF, 40 μM leupeptin) containing PBS. After sonication, aliquots containing 50 μg of total protein were size-fractionated by SDS-PAGE (5–20% gradient gels), and the proteins were transferred to polyvinylidine difluoride membranes (Immobilon, Millipore, Bedford, MA) as described previously.[25] The membranes were blocked with 5% skim milk and

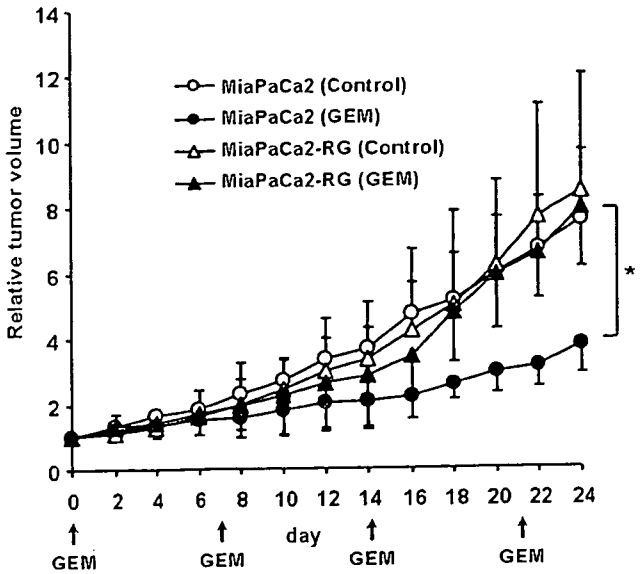

FIGURE 2 – *In vivo* gemcitabine sensitivity of MiaPaCa2 and MiaPaCa2-RG in subcutaneous xenograft model of nude mice. Gemcitabine was injected weekly into the peritoneal cavity at the dose of 240 mg/kg (closed circle and closed triangle) and control (open circle, open triangle). Points, mean; bars, SD ($n = 5$). *$p < 0.01$.

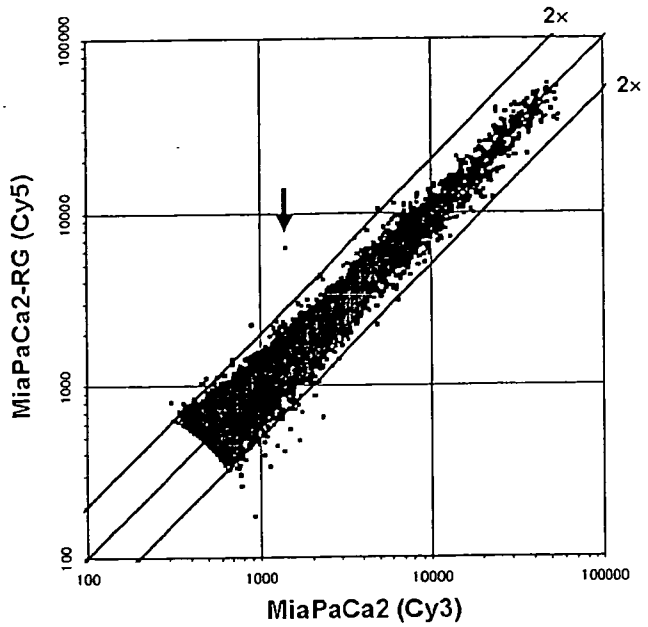

FIGURE 3 – Representative scatterplots showing hybridizations of cDNA from MiaPaCa2 cells labeled Cy3 and MiaPaCa2-RG cells labeled Cy5. The lines show 2-fold difference expression in both channels. RRM1; arrow.

incubated for 1 hr at room temperature with mouse monoclonal anti-human RRM1 (Chemicon international, Inc., Temecula, CA) or rabbit polyclonal anti-human actin (Sigma). After 3 washings with 0.1% Tween 20 in TBS, the membranes were incubated for 30 min at room temperature with the horseradish peroxidase-conjugated secondary antibody. After further 5 washings peroxidase was detected with an enhanced chemiluminescence system from Amersham (Arlington Heights, IL).

RNAi treatment

RRM1 and control RNAis were purchased from Invitrogen (Stealth RNAi; Invitrogen, Carlsbad, CA). The RRM1-specific RNAi designed by BLOCK-iT RNAi Designer (Invitrogen, Carlsbad, CA) was as follows: Sense 5′-GGAUAUUGUUCUGGCCAAUAAAGAU-3′; Anti-sense 5′-AUCUUUAUUGGCCAGAACAAUAUCC-3′. A stealth RNAi negative control with medium GC duplex was used as a control. RNAis were dissolved in DEPC-treated water to make a 20 μM working stock. One day before transfection, 2×10^5 cells were plated into 35 mm, 6-well trays and allowed to adhere. Transfection was performed using Lipofectamine 2000 transfection regent (Invitrogen, Carlsbad, CA) following Invitrogen's protocols. The ability of the RNAi molecules to knock down RRM1 expression was analyzed by mRNA and protein detection, and the final dilution volume of RNAi was 50 pmol in 500 μl OptiMEM medium per well.

Patients and tissue samples

Eighteen recurrent pancreatic cancer patients in Osaka University Hospital were recruited. All patients had undertaken curative resection at Osaka University Hospital between September 1999 and February 2004 and were followed-up without any adjuvant treatment until recurrence. The tumor tissues had been collected and stored at −80°C until use under informed written consent. Each tumor was confirmed histopathologically to be advanced stage cancer. All patients had a measurable recurrent lesion and were treated with only gemcitabine after recurrence. Response to gemcitabine was defined as follows: complete response (CR), partial response (PR), stable disease (SD) and progressive disease (PD). This classification was based on New Guidelines to Evaluate the Response to Treatment in Solid Tumors (RECIST guidelines).[30] Patients were divided into 2 groups based on the chemotherapeutic response. Responders were defined as CR, PR and SD. Nonresponders were PD. A total of 18 tumor samples resected at the primary curative operation were analyzed to determine RRM1 mRNA expression levels. Total RNA was isolated from the homogenate tumor samples using TRIzol method[27] for quantitative reverse transcription-polymerase chain reaction (RT-PCR) using same conditions as already described. Total RNA of MiaPaCa2-RG was used for analytical curve.

Statistical analysis

Statistical analyses were performed using the SPSS 11.5J software (SPSS Inc., Chicago, IL). All data were expressed as mean ± SD. Differences between groups were examined for statistical significance using the Student's t test. In the clinical study, associations between the candidate molecule expression and gemcitabine response were assessed by Fisher's exact test. Overall, survival probabilities were estimated using the Kaplan-Meier method, and the log-rank test was used to determine the level of significance between the survival curves. A p value less than 0.05 denoted the presence of a statistically significant difference.

Results

Establishment of gemcitabine-resistant pancreatic cancer cell lines

Three types of pancreatic cancer cell lines, BxPC3, PSN1 and MiaPaCa2, were cultured in the medium containing gemcitabine for 2 months. After selection, we established 3 variant cells resistant to gemcitabine with different degrees with the MTT assay (Table I). The selected cell lines were called BxPC3-RG, MiaPaCa2-RG or PSN1-RG, based on the names of their parental cell line. On the basis of the IC_{50} measurement, BxPC3-RG, MiaPaCa2-RG and PSN1-RG were 11-fold, 81-fold and 986-fold more resistant than parental cells to the cytotoxic effects of gemcitabine, respectively. BxPC3-RG and PSN1-RG were also cross-resistant to 5-FU, although MiaPaCa2-RG represented no significant

TABLE II – GENES UP- AND DOWNREGULATED BY MORE THAN 2-FOLD IN MiaPaCa2-RG WITH MIAPACA2 AS A REFERENCE

	Fold	Gene name	Symbol	Accession no.
Upregulated				
1	4.46	Ribonucleotide reductase m1 polypeptide	RRM1	NM_001033
2	2.63	ensembl genscan prediction		AL050329
3	2.29	kiaa0101 gene product	KIAA0101	NM_014736
4	2.27	Hypothetical protein	ATP5S	NM_015684
5	2.20	Inosine monophosphate dehydrogenase 1	IMPDH1	XM_004627
6	2.19	Hypothetical protein flj20558	FLJ20558	NM_017880
7	2.09	Suppression of tumorigenicity 7	ST7	NM_018412
8	2.07	Hypothetical protein xp_040263	LOC91732	XM_040263
9	2.06	Suppressor of g2 allele of skp1	SUGT1	NM_006704
10	2.02	Unknown (protein for image:3456579)	FUBP3	BC001325
11	2.00	ba196n14.4.1 (pro1085 protein, isoform 1)		AL354776
12	2.00	Hypothetical protein xp_039528	LOC91613	XM_039528
Downregulated				
1	5.32	ensembl genscan prediction		AC063943
2	3.50	Antiquitin	ALDH7A1	NM_001182
3	3.49	ensembl genscan prediction		AC068601
4	3.36	Adenylate cyclase 6, isoform b	ADCY6	NM_020983
5	3.31	ensembl genscan prediction		AC009294
6	3.01	Activator of s phase kinase	ASK	NM_006716
7	2.78	udp glycosyltransferase 2 family, polypeptide b4	UGT2B4	NM_021139
8	2.69	ensembl genscan prediction		AF131216
9	2.66	ensembl genscan prediction		AF277315
10	2.54	Unknown	C9orf10	AF055017
11	2.48	Potassium voltage-gated channel, shal-related subfamily, member 3	KCND3	NM_004980
12	2.34	ensembl genscan prediction		AC005034
13	2.29	ensembl genscan prediction		AL356751
14	2.26	ensembl genscan prediction		AL135978
15	2.23	ensembl genscan prediction		AC021883
16	2.21	Adaptor-related protein complex 2, mu 1 subunit	AP2M1	NM_004068
17	2.21	Phosphoserine phosphatase	PSPH	NM_004577
18	2.18	Transaldolase-related protein	TALDO1	AF010400
19	2.16	Hypothetical protein xp_016148	LOC95556	XM_016148
20	2.15	Transcription elongation factor a (sii), 1	TCEA1	NM_006756
21	2.14	Hepatitis a virus cellular receptor 1	HAVCR1	NM_012206
22	2.13	Protein phosphatase 1, regulatory (inhibitor) subunit 2	PPP1R2	NM_006241
23	2.12	Ring finger protein 22, isoform beta	TRIM3	NM_033278
24	2.11	Glycine cleavage system protein h	GCSH	NM_004483
25	2.07	Hypothetical protein nuf2r	CDCA1	BC008489
26	2.06	Dj1093g12.6 (a novel protein)	C20orf93	AL121751
27	2.05	Inosine-5′-monophosphate dehydrogenase	IMPDH2	J04208
28	2.02	Hypothetical protein xp_052919	LOC112547	XM_052919
29	2.02	ensembl genscan prediction		AL132801
30	2.01	ensembl genscan prediction		AC010553
31	2.00	Heme-regulated initiation factor 2-alpha kinase	HRI	NM_014413

cross-resistance (Table I). By the growth curve analysis, MiaPaCa2-RG and PSN1-RG showed significant resistant to gemcitabine, although BxPC3-RG did not show any resistance to gemcitabine. In the absence of gemcitabine, BxPC3-RG and MiaPaCa2-RG demonstrated almost the same growth curves when compared with parental cells, although PSN1-RG's growth rate was 10-fold slower than PSN1 (Fig. 1*a*). BxPC3-RG and MiaPaCa2-RG preserved the cell morphology of parental cells regardless of these chemoresistant alterations, and PSN1-RG showed significant difference in the cell morphology (Fig. 1*b*). MiaPaCa2-RG remained gemcitabine-resistant after 1 month culture in the medium without gemcitabine. Furthermore, MiaPaCa2-RG showed significant gemcitabine-resistance when compared with MiaPaCa2 in an *in vivo* xenograft model (Fig. 2). The level of [^{3}H] gemcitabine cellular uptake in MiaPaCa2-RG (25.0 ± 3.2 pg GEM/μg protein) is half of that in MiaPaCa2 (49.9 ± 5.8 pg GEM/μg protein). These data suggest that MiaPaCa2-RG should be the most suitable for identifying genetic alterations relating to gemcitabine resistance among the 3 types of gemcitabine-selected variants. We chose MiaPaCa2-RG for further analysis to identify molecules associated with gemcitabine resistance.

Microarray analysis

To investigate the candidate genes involved in gemcitabine resistance, oligo-microarray experiments were carried out with MiaPaCa2 and MiaPaCa2-RG cells. Out of the 30,000 spotted genes, 10,517 genes were used for further analysis (See Material and methods). Scatter plotting showed that 99.6% genes (10,474 genes out of 10,517 genes) had altered expressions of less than 2-fold, and 43 genes were up- or downregulated more than 2-fold in MiaPaCa2-RG cells when compared with MiaPaCa2 cells (Fig. 3). Among the 43 genes in which 12 upregulated genes and 31 downregulated genes were identified, the RRM1 was the most upregulated with 4.5-fold (Table II). This gene is the subunit of ribonucleotide reductase (RR) considered as an enzyme associated with gemcitabine metabolism.[4] This upregulation was validated by both quantitative RT-PCR and Western blotting (data not shown). Other subunits of RR, RRM2 and p53R2, and other enzymes involved in gemcitabine metabolism such as CDA, dCK, CTP synthetase and dCMP deaminase and nucleotide transporters were not chosen in the microarray analysis because of their low expression levels or failure to show any altered expression between MiaPaCa2 and MiaPaCa2-RG with quantitative RT-PCR. The func-

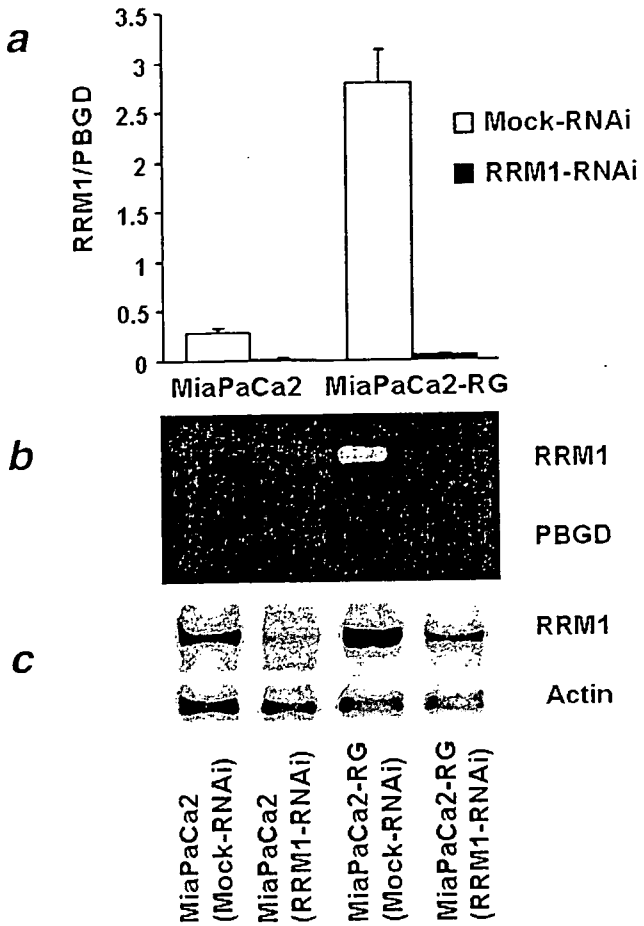

FIGURE 4 – (*a*) Quantitative RT-PCR, (*b*) RT-PCR and (*c*) Western blotting analyses of RRM1 expression after RRM1-specific RNAi transfection in MiaPaCa2 and MiaPaCa2-RG cells. Columns, mean; bars, SD ($n = 3$).

tions of other up- and downregulated genes were not considered to have any association with gemcitabine sensitivity. Therefore, we focused on the RRM1 gene for further functional analysis.

Chemosensitivity after RRM1-specific RNAi transfection

To verify that RRM1 should be involved in gemcitabine resistance, RNAi experiments were carried out on MiaPaCa2 and MiaPaCa2-RG. The ability of RRM1-specific RNAi to suppress RRM1 expression was confirmed by both RT-PCR (Figs. 4*a* and 4*b*) and Western blotting (Fig. 4*c*). After transfection with RRM1-specific RNAi, more than 90% suppression of RRM1 was observed (Fig. 4*a*). Other subunits of ribonucleotide reductase, RRM2 and p53R2, did not have any significant mRNA expression change. RRM1-specific RNAi transfection did not bring about any major effect on cell viability. After RRM1-specific RNAi transfection, the gemcitabine chemoresistance of MiaPaCa2-RG was significantly reduced to same level as that of MiaPaCa2, and gemcitabine response of MiaPaCa2 also became more sensitive (Fig. 5).

RRM1 expression and gemcitabine response in human pancreatic cancer cells and patients with pancreatic cancer

To investigate that the increased expression also should be involved in intrinsic resistance to gemcitabine, we examined the association between RRM1 mRNA expression levels and gemcitabine sensitivity of 5 human pancreatic cancer cell lines at first. RRM1 mRNA expression levels are significantly associated with gemcitabine sensitivity in 5 pancreatic cancer cell lines (Fig. 6), although increased expression of RRM1 was not likely correlated with the increase of cellular resistance to gemcitabine between acquired gemcitabine resistant MiaPaCa2-RG cells and PSN1-RG cells. Next, we examined the correlation of RRM1 mRNA expression levels with clinical course of 18 patients with recurrent pancreatic cancer. Seven patients developed liver metastasis, 4 developed local recurrence, 3 developed lymph node metastasis, 2 developed lung metastasis and 2 developed multi site recurrence (1 patient had local recurrence and liver metastasis and the other had liver, lung, bone and lymph node metastasis). The response to gemcitabine were CR ($n = 0$), PR ($n = 2$), SD ($n = 6$) and PD ($n = 10$). We classified 8 patients as responders (PR and SD) and 10 patients as nonresponders (PD). On the other hand, the median RRM1 mRNA expression relative to the housekeeping gene PBGD was 1.3×10^{-2} (minimum expression, 0.0×10^{-2}; maximum expression, 132.0×10^{-2}) in 18 pancreatic tissue samples (Fig. 7). According to a cut-off value of 1.3×10^{-2}, 9 patients (50%) were classified into the low RRM1 expression group, and 9 patients (50%) into the high RRM1 expression group. There was a significant association between gemcitabine response and RRM1 expression ($p = 0.018$) (Table III). Furthermore, patients with

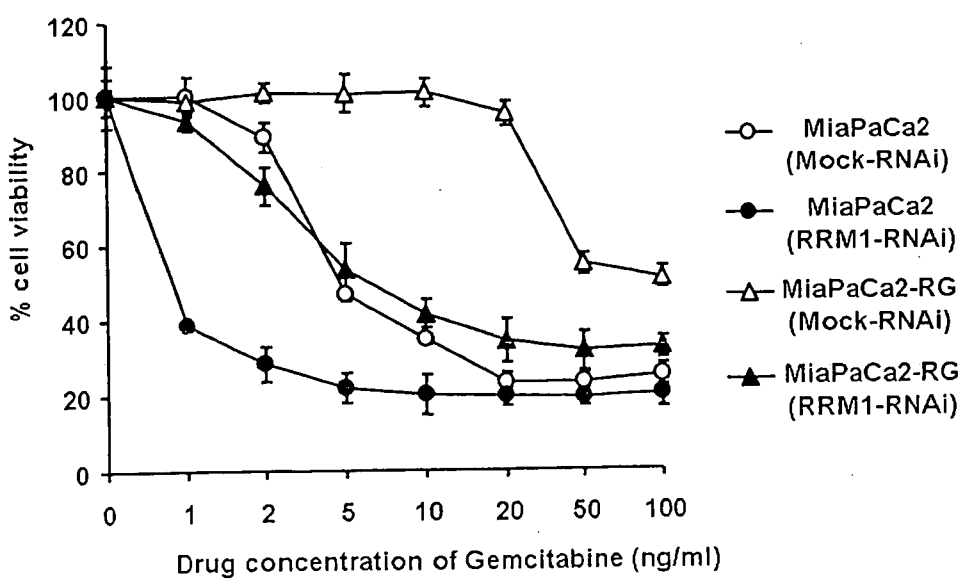

FIGURE 5 – Dose–response curves for gemcitabine in MiaPaCa2 (circle) and MiaPaCa2-RG (triangle) after RNAi transfection. Open circles and triangles indicate mock RNAi transfectant. Closed circles and triangles indicate RRM1-specific RNAi transfectant. Points, mean; bars, SD ($n = 3$).

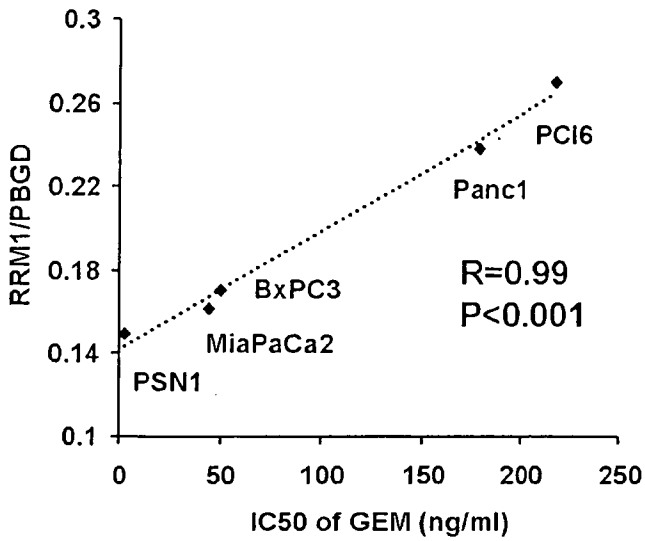

FIGURE 6 – Correlation of gemcitabine sensitivity with RRM1 expression in 5 human pancreatic cancer cell lines ($n = 3$). $R = 0.99$, $p < 0.001$.

high RRM1 levels had poor survival times after gemcitabine treatment than those with low RRM1 levels (Fig. 8; $p = 0.016$). Median survival times after gemcitabine treatment was 6.0 months for patients with high RRM1 levels and 14.6 months for patients with low levels.

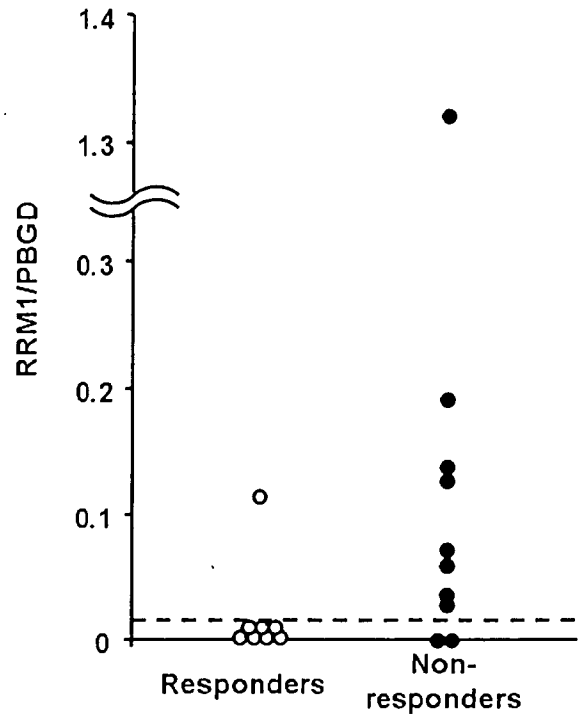

FIGURE 7 – RRM1 expression levels classified by gemcitabine response in the human pancreatic cancer tissues. Dotted bar: RRM1 cut-off value of 1.3×10^{-2}.

TABLE III – ASSOCIATION BETWEEN GEMCITABINE RESPONSE AND RRM1 mRNA EXPRESSION LEVELS

	RRM1 level[1]		
	High	Low	Total
Responder (PR, SD)	1	7	8
Nonresponder (PD)	8	2	10
Total	*9*	*9*	*18*

Fisher's exact test, $p = 0.018$.
[1]Cut-off value is median RRM1 expression relative to PBGD (1.3×10^{-2}).

Discussion

The present study have demonstrated that RRM1, which is a subunit of ribonucleotide reductase (one of the key enzymes in gemcitabine metabolism), should be clearly involved in gemcitabine resistance in human pancreatic cancer. First, oligonucleotide microarray analysis covering 30,000 human oligonucleotides between human pancreatic cancer cells resistant to gemcitabine and parental cells demonstrated that the most upregulated gene in the gemcitabine-resistant variant MiaPaCa2-RG cells was the RRM1 gene. RRM1 expression in the resistant cells was 4.5-fold higher than parental cells. This up-regulation was validated by quantitative RT-PCR and Western blotting. Furthermore, there was no difference between the expression levels of the other subunits of ribonucleotide reductase or the other molecules in gemcitabine metabolism including dCK, CTP synthetase, dCMP deaminase and nucleotide transporters. Second, by RRM1-specific RNAi transfection, RRM1 expression in both mRNA and protein levels were significantly decreased and the gemcitabine chemoresistance of MiaPaCa2-RG was significantly reduced to same level as that of MiaPaCa2. Third, the most important point was confirmation by the clinical analysis. Increased RRM1 expression was significantly associated with antitumor effects and with poor survival after treatment with gemcitabine in pancreatic cancer patients ($p = 0.018$ and 0.016, respectively). Therefore, RRM1 could be the targeted molecule to regulate gemcitabine resistance. Furthermore, its expression levels could be a useful indicator of gemcitabine resistance.

Ribonucleotide reductase (RR) acts as the rate-limiting enzyme in *de novo* DNA synthesis, because it is the only known enzyme that converts ribonucleotides to deoxyribonucleotides, which step is mandatory for DNA polymerization and repair.[31,32] In the cell, a deoxycytidine analogue, gemcitabine, is phosphorylated to monophosphate, diphosphate, and triphosphate before incorporation into DNA, which is required for its growth inhibiting activity. The diphosphorylated form of gemcitabine acts as a RR inhibitor, and some of gemcitabine cytotoxic activity is due to this inhibition.[33] Ribonucleotide reductase increases the deoxynucleoside triphosphate (dNTP) pool in the cells, which could lead to decreased incorporation of dNTP analogues such as triphosphorylated gemcitabine into DNA and might reduce the antitumor effect of gemcitabine.[22] In fact, MiaPaCa2-RG, higher expresser of RRM1 mRNA, showed lower gemcitabine uptake than lower RRM1 expresser MiaPaCa2.

Recent results have shown that there are 3 human ribonucleotide reductase subunits: RRM1, RRM2 and p53R2. RRM1 is a large peptide chain (α), and RRM2 and p53R2 are small protein subunits of RR (β). The catalytically active form of eukaryotic ribonucleotide reductase is proposed to be a $\alpha_2\beta_2$ heterotetrameter made up of 2 large subunits and 2 small subunits.[34,35] Although ribonucleotide reductase enzymatic activity is modulated by levels of RRM2[36] and p53R2,[37] RRM1 could play a key role among the 3 subunits in the course of gemcitabine treatment. RRM1 controls substrate specificity and global on/off enzyme activity.[36,37] As suggested by Davidson *et al.*, RRM1 could act as a "molecular sink" for gemcitabine, in which RRM1 binds irreversibly to the drug and inactivates it, while increased RRM1 expression did not alter ribonucleotide reductase activity in the gemcitabine resistant variant human lung cancer cells.[12] RRM1 was upregulated in the 2 selected gemcitabine resistant human lung cancer cell lines, where RRM1 expression levels were correlated with gemcitabine concentration for cell selection.[12] A recent microarray analysis

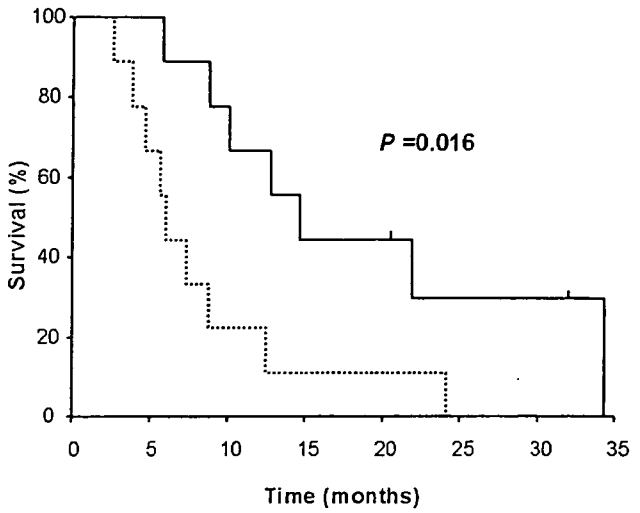

FIGURE 8 – Overall survival after gemcitabine treatment of 18 recurrent pancreatic cancer patients for RRM1 mRNA expression levels. Solid line: low RRM1 expression group (n = 9). Dotted line: high RRM1 expression group (n = 9). Log-rank test = 5.78, p =0.016.

has suggested that *in vivo* induction of resistance to gemcitabine should result in increased expression of RRM1.[13] These data are consistent with the present findings, although they only suggested an association of gemcitabine resistance with higher RRM1 expression. More important was the clear demonstration in the present study of the direct association of RRM1 with gemcitabine resistance through RRM1-specific RNAi treatment. However, the precise mechanisms how the increased expression of RRM1 acts in gemcitabine resistance still remain obscure. In the *in vitro* study with acquired gemcitabine resistant MiaPaCa2-RG and PSN1-RG cells, increase expression of RRM1 was not likely correlated with the increase of cellular resistance to gemcitabine. Although gemcitabine-resistance of PSN1-RG cells was almost equal to that of MiaPaCa2-RG cells, RRM1 expression level was much higher in MiaPaCa2-RG than in PSN1-RG cells. Other molecules involving gemcitabine or 5-FU metabolism or molecules such as p8[38] may be participated in gemcitabine resistance. Further studies are needed to clarify these points.

Although association of the increased expression of RRM1 gene with gemcitabine resistance has been reported based on *in vitro* and *in vivo* acquired gemcitabine resistant tumor cells[12,13] as in the present study, the mechanisms under RRM1 upregulation of resistant cells have not been fully elucidated. Polymorphisms[39] and amplified gene copy number[40] in the RRM1 gene are supposed to be related to the gemcitabine chemoresistance of tumor cells. Gene mutation or epigenetic mechanism such as methylation may influence the expression of RRM1 in resistant cells. Our preliminary experiments, however, did not show any mutational or polymorphic changes in the RRM1 gene between parental and gemcitabine resistant selected cells. Demethylation agents such as 5-aza-2′-deoxycytidine did not change RRM1expression in gemcitabine resistant cells. Future studies for the regulation of RRM1expression could therefore be helpful to obtain modulation of gemcitabine sensitivity in pancreatic cancer cells.

Because the present findings on RRM1 as a factor in gemcitabine resistance are based on an *in vitro* acquired gemcitabine resistant model as shown in the previous studies,[12] it is still unclear whether or not RRM1 should be one of the key molecules involved in the intrinsic resistance to gemcitabine. However, in *in vitro* analysis with human pancreatic cancer cell lines, RRM1 mRNA expression levels are significantly associated with gemcitabine sensitivity in 5 pancreatic cancer cell lines, while increased expression of RRM1 was not likely correlated with the increase of cellular resistance to gemcitabine between acquired gemcitabine resistant MiaPaCa2-RG cells and PSN1-RG cells. Furthermore, clinical data from patients treated with gemcitabine may indicate that RRM1 should play an important role in the intrinsic resistance to gemcitabine. Gemcitabine was more effective to recurrent tumors in those patients with low RRM1 mRNA expression in the tumor obtained at surgery, although expression levels of recurrent tumors were supposed to reflect those of primary tumors. Therefore, patients with low RRM1 mRNA expression might have a significantly longer survival than those with a high expression as previously reported in lung cancer patients[41,42] even though the survival of recurrent pancreatic cancer patients is generally poor. Although our data do not rule out that other molecules of gemcitabine resistance determine intrinsic or acquired sensitivity to gemcitabine *in vivo* as reported in the recent study, the clinical results should be the most feasible for further investigations.

In conclusion, we have demonstrated in the present study that RRM1 should be a key molecule in gemcitabine resistance in pancreatic cancer through both *in vitro* and clinical models. In the continuous struggle to overcome the chemoresistance of pancreatic cancer, RRM1 may have the potential to play the role of a predictor of gemcitabine resistance and modulator of gemcitabine treatment.

References

1. Li D, Xie K, Wolff R, Abbruzzese JL. Pancreatic cancer. Lancet 2004;363:1049–57.
2. Burris HA, III, Moore MJ, Andersen J, Green MR, Rothenberg ML, Modiano MR, Cripps MC, Portenoy RK, Storniolo AM, Tarassoff P, Nelson R, Dorr FA, et al. Improvements in survival and clinical benefit with gemcitabine as first-line therapy for patients with advanced pancreas cancer: a randomized trial. J Clin Oncol 1997;15:2403–13.
3. Louvet C, Labianca R, Hammel P, Lledo G, Zampino MG, Andre T, Zaniboni A, Ducreux M, Aitini E, Taieb J, Faroux R, Lepere C, et al. Gemcitabine in combination with oxaliplatin compared with gemcitabine alone in locally advanced or metastatic pancreatic cancer: results of a GERCOR and GISCAD phase III trial. J Clin Oncol 2005;23: 3509–16.
4. Bergman AM, Pinedo HM, Peters GJ. Determinants of resistance to 2′,2′-difluorodeoxycytidine (gemcitabine). Drug Resist Updat 2002;5:19–33.
5. Galmarini CM, Clarke ML, Falette N, Puisieux A, Mackey JR, Dumontet C. Expression of a non-functional p53 affects the sensitivity of cancer cells to gemcitabine. Int J Cancer 2002;97:439–45.
6. Shi X, Liu S, Kleeff J, Friess H, Buchler MW. Acquired resistance of pancreatic cancer cells towards 5-FU and gemcitabine is associated with altered expression of apoptosis-regulating genes. Oncology 2002;62: 354–62.
7. Duxbury MS, Ito H, Zinner MJ, Ashley SW, Whang EE. Inhibition of SRC tyrosine kinase impairs inherent and acquired gemcitabine resistance in human pancreatic adenocarcinoma cells. Clin Cancer Res 2004;10:2307–18.
8. Duxbury MS, Ito H, Benoit E, Zinner MJ, Ashley SW, Whang EE. RNA interference targeting focal adhesion kinase enhances pancreatic adenocarcinoma gemcitabine chemosensitivity. Biochem Biophys Res Commun 2003;311:786–92.
9. Akada M, Crnogorac-Jurcevic T, Lattimore S, Mahon P, Lopes R, Sunamura M, Matsuno S, Lemoine NR. Intrinsic chemoresistance to gemcitabine is associated with decreased expression of BNIP3 in pancreatic cancer. Clin Cancer Res 2005;11:3094–101.
10. Mackey JR, Mani RS, Selner M, Mowles D, Young JD, Belt JA, Crawford CR, Cass CE. Functional nucleoside transporters are required for gemcitabine influx and manifestation of toxicity in cancer cell lines. Cancer Res 1998;58:4349–57.
11. Rauchwerger DR, Firby PS, Hedley DW, Moore MJ. Equilibrative-sensitive nucleoside transporter and its role in gemcitabine sensitivity. Cancer Res 2000;60:6075–9.
12. Davidson JD, Ma L, Flagella M, Geeganage S, Gelbert LM, Slapak CA. An increase in the expression of ribonucleotide reductase large subunit 1 is associated with gemcitabine resistance in non-small cell lung cancer cell lines. Cancer Res 2004;64:3761–6.